Inorg. Chem. **2008**, *47*, 8957−8971

Anion-Dependent Self-Assembly of Silver(I) and Diaminotriazines to Coordination Polymers: Non-Covalent Bonds and Role Interchange between Silver and Hydrogen Bonds

Blanca R. Manzano,*,† Félix A. Jalón,† M. Laura Soriano,† M. Carmen Carrión,† M. Pilar Carranza,† Kurt Mereiter,‡ Ana M. Rodríguez,§ Antonio de la Hoz,† and Ana Sánchez-Migallón†

Departamento de Química Inorgánica, Orgánica y Bioquímica, Facultad de Químicas, IRICA, Universidad de Castilla−La Mancha, Avda Camilo José Cela, 10, E-13071 Ciudad Real, Spain, Faculty of Chemistry, Vienna University of Technology, Getreidemarkt 9/164 SC, A-1060 Vienna, Austria, and Departamento de Química Inorgánica, Orgánica y Bioquímica, Escuela Técnica Superior de Ingenieros Industriales, Universidad de Castilla−La Mancha, Avda Camilo José Cela, 3, E-13071 Ciudad Real, Spain

Received May 31, 2008

New coordination polymers have been obtained by the self-assembly of silver salts AgX (X = BF_4, PF_6, CF_3SO_3) and 2,4-diamino-6-R-1,3,5-triazines L (R = phenyl and *p*-tolyl) of formulas AgLX (**1**−**6**). A complex of different stoichiometry, $[Ag_3L_2(H_2O)(acetone)_2](BF_4)_3$, **7** (R = phenyl), has also been synthesized. The three-dimensional structures of five compounds have been determined by X-ray diffraction studies. For the AgLX complexes, when X = BF_4 and R = phenyl or *p*-tolyl, chiral chains with alternating Ag and L are formed. The chains are cross-linked by the counteranions in a three-dimensional fashion through hydrogen bonds and weak Ag···F interactions giving rise to a structure with solvent-filled channels. Different and more compact structures have been found when the counteranion is CF_3SO_3 (OTf). When R = phenyl, sheets are formed which consist of $[Ag_2(OTf)_2L_2]$ units with double triflate bridges and which contain columns of $\pi-\pi$ stacked arenes. Hydrogen bonds connect the sheets. When AgOTf is used and R is *p*-tolyl, a different and unusual ladderlike structure is obtained in which the rungs are double asymmetric bridges consisting of the triflate groups bonded to Ag in κ^2O,μ_2-*O* and κ^1O,μ_2-*O* fashion. The ladders are parallel to each other and are mutually linked by N−H···N hydrogen bonds to give a 3D architecture. A very similar ladderlike structure has been found for **7** but with a water molecule and a BF_4^- group acting as bridges. The role played by the hydrogen bonds in complex **6** to form the 3-D structure is played in **7** by $[Ag(acetone)_2]$ fragments. The noncovalent interactions play an important role in the different solid-state 3D structures. The behavior of the new derivatives in solution has also been analyzed. A new species has been detected at low temperatures, and this exhibits restricted rotation of the phenyl ring.

Introduction

The past few decades have witnessed growing interest and enormous progress in the field of coordination polymers and metal−organic framework (MOF) derivatives.[1] Such materials not only have potential applications as sensors, in gas storage and catalysis, or as optoelectronic and magnetic materials[2] but also exhibit structural and topological novelty with diverse and intriguing structural motifs. The key features that influence the architecture of self-assembled species are the building blocks: the metal, which has a more or less

* Author to whom correspondence should be addressed. Fax: (internat.) + 34-926/295318. E-mail: Blanca.Manzano@uclm.es.
† IRICA, Universidad de Castilla−La Mancha.
‡ Vienna University of Technology.
§ Escuela Técnica Superior de Ingenieros Industriales, Universidad de Castilla−La Mancha.

(1) (a) Leininger, S.; Olenyuk, B.; Stang, P. J. *Chem. Rev.* **2000**, *100*, 853–908. (b) Swiegers, G. F.; Malefetse, T. J. *Chem. Rev.* **2000**, *100*, 3483–3538. (c) Eddaoudi, M.; Moler, D. B.; Li, H.; Chen, B.; Reineke, T. M.; O'Keeffe, M.; Yagi, O. M. *Acc. Chem. Res.* **2001**, *34*, 319–330. (d) Ockwig, N. W.; Delgado-Friedrichs, O.; O'Keeffe, M.; Yagi, O. M. *Acc. Chem. Res.* **2005**, *38*, 176–182. (e) Moulton, B.; Zaworotko, M. J. *Chem. Rev.* **2001**, *101*, 1629–1658. (f) Blake, A. J.; Champness, N. R.; Hubberstey, P.; Li, W.-S.; Withersby, M. A.; Schröder, M. *Coord. Chem. Rev.* **1999**, *183*, 117–138. (g) Hong, M. *Crystal Grow. Des.* **2007**, *7*, 10–14.

10.1021/ic800997d CCC: $40.75
Published on Web 09/10/2008

preferred coordination environment, and the ligand, which not only provides the donor atoms situated at specific positions[3] but can also provide potential interaction sites to generate noncovalent interactions, such as hydrogen-bonding,[4] $\pi-\pi$ stacking,[5] and anion$-\pi$ and C$-$H$\cdots\pi$ interactions.[6] These secondary interactions may be very important for different aspects such as molecular recognition and catalysis and, more specifically, for enantioselective processes.[2g,7]

In metallo-assembled architectures, the dominant factor that controls the final supramolecule is usually the metal$-$ligand interaction, and any structure adopted must fulfill the requirements of the metal ion. With metals lacking strong coordination preferences, a certain number of structures could have similar stabilities, and weak noncovalent interactions may have a strong effect and determine the organization of the complex supramolecular network.[8,9] The main goal of this work was to analyze these noncovalent interactions in order to get a deeper insight of how they can influence the system. In order to get that, we chose the Ag(I) center as the metal building block because it is a cation with modest stereochemical preferences and is adaptable to different coordination geometries.[9,10] In addition, the Ag$-$N bonds are not very strong. It has been reported that the energy of a Ag$-$N(pyridine) bond is similar to that of a strong hydrogen bond.[11] It is also important to note that many silver$-$ligand bonds, among them the Ag$-$N bond, are labile in solution, and this gives rise to reversible processes for supramolecular structure formation.[11] This would lead$-$through a self-correction process[12]$-$toward the thermodynamically more stable architecture, and it is expected that there would also be an influence of different changes such as, for example, the counteranion or small variations in the ligands. Many examples of silver(I) coordination polymers have been described, and these include linear chains, zigzag chains, helices, ladders, and two- and three-dimensional networks of different natures.[1f,11,13] Discrete species of distinct nuclearity have also been reported.[9,14]

As organic synthons, we decided to use 2,4-diamino-6-R-1,3,5-triazines (see Scheme 1), mainly because they could give rise to different types of secondary interactions. It has been reported that the *s*-triazine ring constitutes a remarkable unit for generating supramolecular interactions, namely, coordination bonding, hydrogen bonding, electrostatic and charge-transfer attractions, and aromatic-stacking interac-

Scheme 1

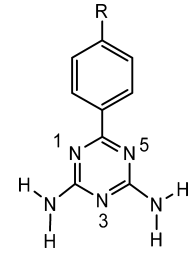

R = H, Phdat
R = Me, Toldat

(2) (a) Holliday, B. J.; Mirkin, C. A. *Angew. Chem., Int. Ed.* **2001**, *40*, 2022–2043. (b) McCleverty, J. A.; Ward, M. D. *Acc. Chem. Res.* **1998**, *31*, 842–851. (c) Gamez, P.; Hoog, P. D.; Roubeau, O.; Lutz, M.; Driessen, W. L.; Spek, A. L.; Reedijk, J. *Chem. Commun.* **2002**, 1488–1489. (d) Hong, M. C.; Zhao, Y. J.; Su, W.; Cao, R.; Fujita, M.; Zhou, Z. Y.; Chan, A. S. C. *Angew. Chem., Int. Ed.* **2000**, *39*, 2468–2470. (e) Yaghi, O. M.; Li, H.; Groy, T. L. *Inorg. Chem.* **1997**, *36*, 4292–4293. (f) Cui, Y.; Ngo, H. L.; Lin, W. B. *Inorg. Chem.* **2002**, *41*, 1033–1035. (g) Würthner, F.; You, C.-C.; Saha-Möller, C. R. *Chem. Soc. Rev.* **2004**, *33*, 133–146. (h) Pri-Bar, I.; Koresh, J. E. *J. Mol. Catal. A: Chem.* **2000**, *156*, 173. (i) Hofmeier, H.; Schubert, U. S. *Chem. Soc. Rev.* **2004**, *33*, 373–399. (j) Rudkevich, D. M. *Angew. Chem., Int. Ed. Engl.* **2004**, *43*, 558–571. (k) Mulfort, K. L.; Hupp, J. T. *J. Am. Chem. Soc.* **2007**, *129*, 9604–9605. (l) Lin, X.; Blake, A. J.; Wilson, C.; Sun, X. Z.; Champness, N. R.; George, M. W.; Hubberstey, P.; Mokaya, R.; Schröder, M. *J. Am. Chem. Soc.* **2006**, *128*, 10745–10753. (m) Jia, J.; Lin, X.; Wilson, C.; Blake, A. J.; Champness, N. R.; Hubberstey, P.; Walker, G.; Cussena, E. J.; Schröder, M. *Chem. Commun.* **2007**, 840–842. (n) Kitagawa, S.; Kitaura, R.; Noro, S.-I. *Angew. Chem., Int. Ed.* **2004**, *43*, 2334–2375. (o) Janiak, C. *Dalton Trans* **2003**, 2781–2804. (p) Uemura, K.; Matsuda, R.; Kitagawa, S. *J. Solid. State Chem.* **2005**, *178*, 2420–2429. (q) Dobrawa, R.; Würthner, F. *J. Polym. Sci., Part A: Polym. Chem.* **2005**, *43*, 4981–4995.

(3) (a) Olenyuk, B.; Fechtenkötter, A.; Stang, P. J. *J. Chem. Soc., Dalton Trans.* **1998**, 1707–1728. (b) Stang, P. J. *Chem.$-$Eur. J.* **1998**, *4*, 19–27. (c) Holliday, B. J.; Mirkin, C. A. *Angew. Chem., Int. Ed.* **2001**, *40*, 2022–2043. (d) Fujita, M.; Umemoto, K.; Yoshizawa, M.; Fujita, N.; Kusukawa, T.; Biradha, K. *Chem. Commun.* **2001**, 509–518. (e) Papaefstathiou, G. S.; MacGillivray, L. R. *Coord. Chem. Rev.* **2003**, *246*, 169–196. (f) Baxter, P. N. M. In *Comprehensive Supramolecular Chemistry*; Atwood, J. L., Davies, J. E. D., MacNicol, D. D., Vögtle, F., Lehn, J.-M., Eds.; Pergamon: Oxford, U. K.; Vol. *9*, pp 165$-$211. Also see Constable, E. C. in the same reference, pp 213$-$252, and Fujita, M. in the same reference, p. 253$-$282. (g) Ward, M. D. *Annu. Rep. Prog. Chem. Sect. A* **2001**, *97*, 293–392.

(4) (a) Jeffrey, G. A. *An Introduction to Hydrogen Bonding*, Oxford University Press, New York, 1997. (b) Beatty, A. M. *Coord. Chem. Rev.* **2003**, *246*, 131–143. (c) Awaleh, M. O.; Badia, A.; Brisse, F. *Cryst. Growth Des.* **2005**, *5*, 1897–1906. (d) Braga, D.; Grepioni, F.; Desiraju, G. R. *Chem. Rev.* **1998**, *98*, 1375–1405.

(5) (a) Janiak, C. *Dalton Trans.* **2000**, 3885–3896, and references therein. (b) Ponzini, F.; Zagha, R.; Hardcastle, K.; Siegel, J. S. *Angew. Chem., Int. Ed.* **2000**, *39*, 2323–2325. (c) Kim, J. L.; Nikolov, D. B.; Burley, S. K. *Nature* **1993**, *365*, 520–527. (d) Kim, Y.; Geiger, J. H.; Hahn, S.; Sigler, P. B. *Nature* **1993**, *365*, 512–520.

(6) (a) Nishio, M.; Umezawa, Y.; Hirota, M.; Takeuchi, Y. *Tetrahedron* **1995**, *51*, 8665–8701. (b) Takahashi, H.; Tsuboyama, S.; Honda, K.; Nishio, M. *Tetrahedron* **2000**, *56*, 6185–6191. (c) Re, S.; Nagase, S. *Chem. Commun.* **2004**, 658–659.

(7) See for example: (a) Pri-Bar, I.; Koresh, J. E. *J. Mol. Catal. A, Chem.* **2000**, *156*, 173–180. (b) van Leeuwen, P. W. N. M.; Roobeek, C. F.; Frijns, J. H. G.; Orpen, A. G. *Organometallics* **1990**, *9*, 1211–1222. (c) Breit, B.; Seiche, W. *J. Am. Chem. Soc.* **2003**, *125*, 6608–6609. (d) Yoshizawa, M.; Tamura, M.; Fujita, M. *Science* **2006**, *312*, 251–254. (e) Wu, C.-D.; Hu, A.; Zhang, L.; Lin, W. *J. Am. Chem. Soc.* **2005**, *127*, 8940–8941. (f) Nishio, M.; Umezawa, Y.; Hirota, M.; Takeuchi, Y. *Tetrahedron* **1995**, *51*, 8665–8701.

(8) Chen, C.-L.; Su, C.-Y.; Cai, Y.-P.; Zhang, H.-X.; Xu, A.-W.; Kang, B.-S.; zur Loye, H.-C. *Inorg. Chem.* **2003**, *42*, 3738–3750.

(9) (a) Hannon, M. J.; Painting, C. L.; Plummer, E. A.; Childs, L. J.; Alcock, N. W. *Chem.$-$Eur. J.* **2002**, *8*, 2225–2238. (b) Price, J. R.; Lan, Y.; Jameson, G. B.; Brooker, S. *Dalton Trans* **2006**, 1491–1494.

(10) (a) Fielden, J.; Long, D.-L.; Slawin, A. M. Z.; Kögerler, P.; Cronin, L. *Inorg. Chem.* **2007**, *46*, 9090–9097. (b) Reger, D. L.; Semeniuc, R. F.; Smith, M. D. *Eur. J. Inorg. Chem.* **2003**, 3480–3494. (c) Blondeau, P.; van der Lee, A.; Barboiu, M. *Inorg. Chem.* **2005**, *44*, 5649–5693.

(11) Khlobystov, A. N.; Blake, A. J.; Champness, N. R.; Lemenovskii, D. A.; Majouga, A. G.; Zyk, N. V.; Schröder, M. *Coord. Chem. Rev.* **2001**, *222*, 155–192.

(12) Stadler, A.-M.; Kyritsakas, N.; Vaughan, G.; Lehn, J.-M. *Chem.$-$Eur. J.* **2007**, *13*, 59–68.

(13) Chen, C.-L.; Kang, B.-S.; Su, C.-Y. *Aust. J. Chem.* **2006**, *59*, 3–18.

(14) (a) Ruben, M.; Rojo, J.; Romero-Salguero, F. J.; Uppadine, L. H.; Lehn, J.-M. *Angew. Chem., Int. Ed.* **2004**, *43*, 3644–3662. (b) Baxter, P. N. W.; Lehn, J.-M.; Baum, G.; Fenske, D. *Chem.$-$Eur. J.* **2000**, *6*, 4510–4517.

tions.[15] The presence of the amino groups could enhance the formation of hydrogen bonds either with the nitrogen atoms of the ring or with other atoms such as, for example, those of the counteranions. The ligands also contain an aromatic substituent in position 6 of the triazine ring, and this could play different roles in the structure and packing of the new compounds through, for example, stacking or hydrophobic interactions. The structures of some of these types of triazine derivatives have been described previously (R = 4-pyridyl,[16] phenyl,[17] 1-piperidino,[17] and 1-phenylpyrazol-3-yl[17]) in addition to that of 6,6′,6″-(1,3,5-phenylene)tris-1,3,5-triazine-2,4-diamine.[18] The supramolecular structure is strongly dependent on the nature of the substituent in position 6. In these structures the molecules are connected through bidirectional N−H···N hydrogen-bonded pairs to form ribbons or sheets that are linked to give a 3D network. The interaction with other organic entities that contain complementary functional groups to form triple hydrogen bonds (DAD/ADA, D = donor of hydrogen, A = acceptor of hydrogen) has been described,[19] but their coordination chemistry has been scarcely explored. Several derivatives in which the diaminotriazine ligand is coordinated by one nitrogen atom of the ring have been described.[20] However, examples involving coordination of the amino nitrogens have not been reported. This is not unexpected considering the acidity of the electron-poor triazine ring. Consequently, the atoms that should be able to coordinate to the metallic center are the three nitrogen atoms of the ring, and according to symmetry arguments, there are two types of these. The coordination of two of these atoms to linear silver cations will give rise to the formation of zigzag chains.

Taking into account the previous considerations on the two building blocks, we consider that our system is very well suited for the study of the effect that the noncovalent interactions have on the final architecture. We were also interested in studying the impact of the counteranion, and we introduced PF_6^-, BF_4^-, and $CF_3SO_3^-$ (OTf) into the system. We envisaged that the coordinating ability of the counterion could play a very important role. In this sense, PF_6^- and BF_4^- will not tend to coordinate easily, and although the triflate anion has sometimes been considered as a poor ligand, its coordination chemistry is now quite broad,[21] and many different types of coordination from monodentate,[22] bidentate,[23] and up to μ_4[24,25] and μ_5[25] are known. The ability of the counterions to form hydrogen bonds was also expected to be important, and once again, the triflate counteranion is expected to have a higher tendency to form such interactions than the other anions.[26,27]

Experimental Section

Materials and Methods. All reactions were carried out under a nitrogen atmosphere using standard Schlenk techniques. All solvents were freshly distilled. AgX (X = BF_4, PF_6, and CF_3SO_3) and Toldat were purchased from Aldrich and used without further purification. The ligand Phdat was prepared by a literature method.[17] Elemental analyses were performed with a Thermo Quest FlashEA 1112 microanalyzer. IR spectra were recorded as Nujol mulls with a Perkin-Elmer PE 883 IR (4000−400 cm^{-1}) or with an ATR system in IRPRESTIGE-21 Shimadzu (4000−700 cm^{-1}) spectrometers. The mass spectrometery measurements were made with a matrix-assisted laser desorption ionization−time of flight (MALDI-TOF) Applied Biosystems Voyager DE STR or with a Q-q-TOF hybrid analyzer with an electrospray ionization source (QStar Elite Applied Biosystems spectrometers). X-ray powder patterns were recorded with Bruker D8 Advance and Panalytical X'Pert MPD diffractometers with Cu Kα radiation. Thermogravimetric analysis (TGA) and differential thermal analysis (DTA) were made with an ATD-TG SETARAM apparatus with a 92−16.18 graphite oven and CS32 controller. The analyses were made with a heating rate of 5 °C/min, under an argon flux in a platinum crucible. ^1H, $^{13}C\{^1H\}$, and ^{19}F NMR spectra were recorded on a Varian Unity 300, a Varian Gemini 400, and an Inova 500 spectrometer. Chemical shifts (ppm) are relative to tetramethylsilane (^1H, ^{13}C NMR) and $CFCl_3$ (^{19}F NMR). Coupling constants (*J*) are in Hertz. The nuclear Overhauser effect difference spectra were recorded with a 5000 Hz spectrum width, an acquisition time of 3.27 s, a pulse width of 90°, a relaxation delay of 4 s, an irradiation power of 5 × 10 dB, and a number of scans of 240. For $^1H-^{13}C$ gradient-selected heteronuclear multiple quantum coherence (g-HMQC) spectra, the standard Varian pulse sequences were used (VNMR 6.1 C software). The spectra were acquired using 7996 Hz (^1H) and 25133.5 Hz (^{13}C) widths; 16 transients of 2048 data points were collected for each of the 256 increments. For variable-temperature spectra, the probe temperature (±1 K) was controlled by a standard unit calibrated with a methanol reference. The carbon resonances are singlets. *o*, *m*,

(15) (a) Gamez, P.; Reedijk, J. *Eur. J. Inorg. Chem.* **2006**, 29–42. (b) Mooibroek, T. J.; Gamez, P. *Inorg. Chim. Acta* **2007**, *360*, 381–404. (c) Ohmori, O.; Kawano, M.; Fujita, M. *Cryst. Eng. Commun.* **2005**, *7*, 255–259. (d) Yamauchi, Y.; Yoshizawa, M.; Fujita, M. *J. Am. Chem. Soc.* **2008**, *130*, 5832–5833.

(16) Chan, C.-W.; Mingos, M. P.; White, A. J. P.; Williams, D. J. *Polyhedron* **1996**, *15*, 1753–1767.

(17) Díaz-Ortiz, A.; Elguero, J.; Foces-Foces, C.; de la Hoz, A.; Moreno, A.; Mateo, M. C.; Sánchez-Migallón, A.; Valiente, G. *New. J. Chem.* **2004**, *28*, 952–958.

(18) Helzy, F. H.; Maris, T.; Wuest, J. D. *Cryst. Growth Des.* **2008**, *8*, 1547–1553.

(19) (a) Bishop, M. M.; Lindoy, L. F.; Skelton, B. W.; White, A. H. *J. Chem. Soc., Dalton Trans.* **2002**, 377–382. (b) Manzano, B. R.; Jalón, F. A.; Soriano, M. L.; Rodríguez, A. M.; de la Hoz, A.; Sánchez-Migallón, A. *Cryst. Growth Des.* **2008**, *8*, 1585–1594.

(20) (a) Deak, A.; Kalman, A.; Parkanyi, L.; Haiduc, I. *Acta Crystallogr., Sect. B* **2001**, *57*, 303–310. (b) Aoki, K.; Inaba, M.; Teratani, S.; Yamazaki, H.; Miyashita, Y. *Inorg. Chem.* **1994**, *33*, 3018–3020. (c) Drew, M. G. B.; Hill, C.; Hudson, M. J.; Iveson, P. B.; Madic, C.; Youngs, T. G. A. *Dalton Trans.* **2004**, 244–251. (d) Dorta, R.; Stoeckli-Evans, H.; Bodensieck, U.; Süss-Fink, G. *J. Organomet. Chem.* **1998**, *553*, 307–315.

(21) (a) Lawrance, G. A. *Chem. Rev.* **1986**, *86*, 17–33. (b) Côté, A. P.; Shimizu, G. K. H. *Coord. Chem. Rev.* **2003**, *245*, 49–64.

(22) See, for example: (a) Venkataraman, D.; Gardner, G. B.; Lee, S.; Moore, J. S. *J. Am. Chem. Soc.* **1995**, *117*, 11600–11601. (b) Gardner, G. B.; Venkataraman, D.; Moore, J. S.; Lee, S. *Nature* **1995**, *374*, 792–795. (c) Venkataraman, D.; Lee, S.; Moore, J. S.; Zhang, P.; Hirsch, K. A.; Gardner, G. B.; Covey, A. C.; Prentice, C. L. *Chem. Mater.* **1996**, *8*, 2030–2040.

(23) See, for example: (a) Hirsch, K. A.; Wilson, S. R.; Moore, J. S. *J. Am. Chem. Soc.* **1997**, *119*, 10401–10412. (b) Hirsch, K. A.; Wilson, S. R.; Moore, J. S. *Inorg. Chem.* **1997**, *36*, 2960–2968.

(24) Lu, X. L.; Leong, W. K.; Hor, T. S. A.; Goh, L. Y. *J. Organomet. Chem.* **2004**, *689*, 1746–1756.

(25) Côté, A. P.; Ferguson, M. J.; Khan, K. A.; Enright, G. D.; Kulynych, A. D.; Dalrymple, S. A.; Shimizu, G. K. H. *Inorg. Chem.* **2002**, *41*, 287–292.

(26) Reger, D. L.; Watson, R. P.; Gardinier, J. R.; Smith, M. D. *Inorg. Chem.* **2004**, *43*, 6609–6619.

(27) Reger, D. L.; Semeniuc, R. F.; Rassolov, V.; Smith, M. D. *Inorg. Chem.* **2004**, *43*, 537–554.

and *p* stand for ortho, meta, and para, respectively. When numbering the protons or carbons, the primes are used for the tolyl substituent.

X-Ray Structure Determination for 2, 3, 5, 6, and 7. The method for the crystallization of compounds **2**, **3**, **5**, and **6** was solvent counter diffusion of the starting reagents and consisted of the use of three layers of different solvents put in a screw-cap tube according to their density. The tube was charged under an inert atmosphere. The lower layer consisted of a solution of the ligand in the solvent with the largest density. A second layer was put in without any reagent in it, and finally the upper layer contained the AgX salt dissolved in the solvent of lowest density (see each complex for the details).

X-ray data for **2**, **3**, **5**, **6**, and **7** were collected on Bruker APEX CCD area detector diffractometers (SMART APEX for **5** and **7**, X8 APEX II for the rest) with graphite monochromated Mo Kα radiation ($\lambda = 0.71073$ Å) and ω-scan frames covering complete spheres of the reciprocal space. The frame data were integrated using the program SAINT,[28] and an absorption correction was performed with the program SADABS.[29] The software package SHELXTL version 6.10[30] was used for space group determination, structure solution, and refinement by full-matrix least-squares methods based on F^2. All non-hydrogen atoms were refined with anisotropic thermal parameters. Hydrogen atoms were placed in calculated positions and refined as riding. For **2** and **5**, the disordered solvent was squeezed with the program PLATON.[31]

Synthesis of [Ag(Phdat)(PF_6)]$_n$·(CH_2Cl_2)$_{2n}$, 1. Phdat (16.8 mg, 0.09 mmol) and $AgPF_6$ (22.8 mg, 0.09 mmol) were mixed in 30 mL of CH_2Cl_2 at room temperature. The colorless solution was stirred over 12 h, and after that the solution was evaporated to dryness. While the solvent was removed under a vacuum, a solid was progressively appearing. The product was washed with a 1:1 mixture of CH_2Cl_2 and Et_2O (2 × 25 mL) and dried. Complex **1** was obtained as a white powder (35.9 mg, 91%). IR (Nujol mull): ν_{max}/cm^{-1} 3382 (NH_2), 1626, 1581, 1535 and 1506, (C═N) and (C═C); 838 and 557 (PF_6). ^{1}H NMR (300 MHz, [D_6]acetone, 25 °C): δ 8.27 (d, $J = 7.0$ Hz, 2H, H_o), 7.58 (t, $J = 7.3$ Hz, 2H, H_m), 7.50 (t, $J = 7.3$ Hz, 1H, H_p), 7.07 ppm (bs, 4H, NH_2). ^{19}F NMR (282 MHz, [D_6]acetone, 25 °C): δ −73.1 ppm (d, $J = 707$ Hz, PF_6). MALDI-TOF MS: *m*/*z*: 294 [AgL]$^+$ (100%), 481 [AgL_2]$^+$ (36.1%), 590 [Ag_2L_2]$^+$ (7.6%). Elem anal. calcd (%) for $C_9H_9AgF_6N_5P$·2(CH_2Cl_2) (609.9): C, 21.66; H, 2.15; N, 11.48. Found: C, 21.30; H, 1.96; N, 12.00 (CH_2Cl_2 content proven by NMR).

Synthesis of [Ag(Phdat)(BF_4)]$_n$, 2. Phdat (20.6 mg, 0.11 mmol) and $AgBF_4$ (21.4 mg, 0.11 mmol) were mixed in 30 mL of tetrahydrofuran (THF) at room temperature, and a white suspension appeared. After 12 h of stirring, the white solid of **2** was concentrated under a vacuum, separated from the solution by filtration, washed with a 1:1 mixture of CH_2Cl_2 and Et_2O (2 × 20 mL), and dried. Complex **2** was obtained as a white powder (37.4 mg, 89%). Colorless crystals for X-ray diffraction were obtained with the following three layers: CH_2Cl_2 with the ligand, neat THF, and acetone with $AgBF_4$. IR (Nujol mull): ν_{max}/cm^{-1} 3374 (NH_2), 1626, 1581, 1530 and 1505 (C═N) and (C═C), 1020 and 523 (BF_4). ^{1}H NMR (300 MHz, [D_6]acetone, 25 °C): δ 8.26 (d, $J = 7.1$ Hz, 2H, H_o), 7.50 (t, $J = 7.3$ Hz, 2H, H_m), 7.59 (t, $J = 7.5$ Hz, 1H, H_p), 7.10 ppm (bs, 4H, NH_2). ^{19}F NMR (282 MHz, [D_6]acetone, 25 °C): δ −151.9 ppm (s, BF_4). MALDI-TOF MS: *m*/*z* 294 [AgL]$^+$ (100%), 481 [AgL_2]$^+$ (36.9%), 590 [Ag_2L_2]$^+$ (7.2%). Elem anal. calcd (%) for $C_9H_9AgBF_4N_5$ (381.9): C, 28.31; H, 2.38; N, 18.34. Found: C, 28.29; H, 2.58; N, 18.50.

Synthesis of [Ag(Phdat)(OTf)]$_n$, 3. Phdat (20.6 mg, 0.11 mmol) and AgOTf (28.3 mg, 0.11 mg) were mixed in 30 mL of THF at room temperature. Immediately, a white suspension appeared. After 12 h of stirring, the suspension was concentrated under a vacuum, separated from the solution by filtration, washed with a 1:1 mixture of CH_2Cl_2 and Et_2O (2 × 20 mL), and dried. Complex **3** is obtained as a white powder (44.8 mg, 92%). Colorless crystals for X-ray diffraction were obtained with the following three layers: CH_2Cl_2/THF with the ligand, neat acetone, and Et_2O with AgOTf. IR (Nujol mull): ν_{max}/cm^{-1} 3344 (NH_2), 1646, 1561, 1541 and 1512 (C═N) and (C═C), 1000 (CH_{phenyl}), 1296, 1175, 818 and 630 (OTf). ^{1}H NMR (300 MHz, [D_6]acetone, 25 °C): δ 8.29 (d, $J = 7.3$ Hz, 2H, H_o), 7.49 (t, $J = 7.1$ Hz, 2H, H_m), 7.54 (t, $J = 7.3$ Hz, 1H, H_p), 7.02 ppm (bs, 4H, NH_2). ^{19}F NMR (282 MHz, [D_6]acetone, 25 °C): δ −80.2 ppm (s, OTf). MALDI-TOF MS: *m*/*z* 294 [AgL]$^+$ (100%), 481 [AgL_2]$^+$ (37.1%), 443 [AgL(OTf)]$^+$ (3.5%). Elem anal. calcd (%) for $C_{10}H_9AgF_3N_5O_3S$ (444.1): C, 27.04; H, 2.04; N, 15.77. Found: C, 27.15; H, 2.13; N, 15.54.

Synthesis of [Ag(Toldat)(PF_6)]$_n$, 4. Toldat (16.1 mg, 0.08 mmol) was made to react with $AgPF_6$ (20.2 mg, 0.08 mmol) in THF (30 mL) at room temperature. A colorless solution was formed, and after 2 h, it was concentrated, and a white suspension appeared. The product was filtrated, washed with Et_2O (3 × 10 mL), and dried under a vacuum. Complex **4** was obtained as a white solid (29.7 mg, 82%). IR (Nujol mull): ν_{max}/cm^{-1} 3348 (NH_2), 1622, 1564 and 1510 (CN) and (C═C), 829 and 556 (PF_6).^{1}H NMR (300 MHz, [D_6]acetone, 25 °C): δ 8.21 (d, $J = 8.2$ Hz, 2H, H-2′,6′), 7.26 (d, $J = 8.2$ Hz, 2H, H-3′,5′), 6.52 (bs, 4H, NH_2), 2.38 ppm (s, 3H, CH_3). ^{19}F NMR (282 MHz, [D_6]acetone, 25 °C): δ −73.1 ppm (d, $J = 708$ Hz, PF_6). MALDI-TOF MS: *m*/*z* 308 [AgL]$^+$ (100%), 509 [AgL_2]$^+$ (33.5%), 616 [Ag_2L_2]$^+$ (7.0%). Elem anal. calcd (%) for $C_{10}H_{11}AgF_6N_5P$ (454.1): C, 26.45; H, 2.44; N, 15.42. Found: C, 26.41; H, 2.50; N, 15.64.

Synthesis of [Ag(Toldat)(BF_4)]$_n$, 5. Toldat (38.2 mg, 0.19 mmol) and $AgBF_4$ (37.0 mg, 0.19 mmol) were mixed in THF (30 mL) at room temperature, and a white suspension was formed. After 2 h, the precipitate was filtered off and washed with Et_2O (3 × 10 mL), then dried under a vacuum. Complex **5** was obtained as a white solid (65.3 mg, 87%). Colorless single crystals of **5** for the X-ray diffraction were obtained after slow diffusion of the reactants using the following three layers: CH_2Cl_2/THF with the ligand, neat THF, and acetone/pentane with $AgBF_4$. IR (Nujol mull): ν_{max}/cm^{-1} 3371 (NH_2), 1626, 1581, 1530 and 1505 (C═N) and (C═C), 1020 and 522 (BF_4). ^{1}H NMR (300 MHz, [D_6]acetone, 25 °C): δ 8.15 (d, $J = 8.3$ Hz, 2H, H-2′,6′), 7.30 (d, $J = 8.3$ Hz, 2H, H-3′,5′), 7.04 (bs, 4H, NH_2), 2.39 (s, 3H, CH_3). ^{13}C {^{1}H} NMR (75 MHz, [D_6]acetone, 25 °C): δ 170.1 (C-2,4), 165.4 (C-6), 129.8 (C-3′,5′), 127.5 (C-2′,6′), 143.0 (C-6′), 135.6 (C-4′), 20.9 ppm (*C*H_3). ^{19}F NMR (282 MHz, [D_6]acetone, 25 °C): δ −151.5 (s, BF_4). ESI-TOF MS: *m*/*z* 107 [Ag]$^+$ (20.8%), 202 [L]$^+$ (100%), 308 [AgL]$^+$ (92.1%), 326 [AgL(H_2O)]$^+$ (16.85%), 509 [AgL_2]$^+$ (35.1%), 616 [Ag_2L_2]$^+$ (7.6%). Elem anal. calcd (%) for $C_{10}H_{11}AgBF_4N_5$ (395.9): C, 30.34; H, 2.80; N, 17.69. Found: C, 30.28; H, 3.01; N, 17.87.

Synthesis of [Ag(Toldat)(OTf)]$_n$, 6. Toldat (22.1 mg, 0.11 mmol) and AgOTf (28.3 mg, 0.11 mmol) were mixed in acetone

(28) Area-Detector Integration Program: *SAINT*+, v. 7.12a; Bruker-Nonius AXS: Madison, WI, 2004.
(29) A Program for Empirical Absorption Correction: Sheldrick, G. M. *SADABS*, version 2004/1; University of Göttingen: Göttingen, Germany, 2004.
(30) (a) Structure Determination Package: *SHELXTL-NT*, version 6.12; Bruker-Nonius AXS: Madison, WI, 2001. (b) SHELXS-97, Program for Structure Solution: Sheldrick, G. M. *Acta Crystallogr., Sect. A* **1990**, *46*, 467. (c) Program for Crystal Structure Refinement: Sheldrick, G. M. *SHELXL-97*; Universität Göttingen: Göttingen, Germany, 1997.
(31) A multipurpose crystallographic tool: Spek, A. L. *PLATON*; Utrecht University: Utrecht, The Netherlands, 2007.

Scheme 2

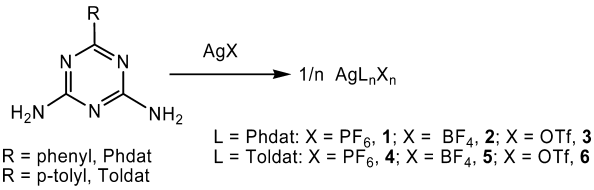

(20 mL) at room temperature, and a white suspension was formed. The reaction was allowed to proceed for 24 h without any further changes. The precipitate was filtered and washed with Et_2O (2 × 10 mL) and then dried under a vacuum. Complex **6** was obtained as a white solid (45.3 mg, 90%). Colorless single crystals of **6** for X-ray diffraction were obtained after slow diffusion of the reactants using the following three layers: CH_2Cl_2/THF with the ligand, neat THF, and acetone/pentane with AgOTf. IR (ATR): ν_{max}/cm^{-1} 3329 (NH_2), 1643, 1612, 1574 and 1530 (C═N) and (C═C); 1299, 1183 and 808 (OTf). ^1H NMR (300 MHz, [D_6]acetone, 25 °C): δ 8.18 (d, J = 8.2 Hz, 2H, H-2′,6′), 7.29 (d, J = 8.2 Hz, 2H, H-3′,5′), 6.91 (bs, 4H, NH_2), 2.39 (s, 3H, CH_3). ^{13}C {^1H} NMR (75 MHz, [D_6]acetone, 25 °C): δ 128.3 (C-2′,6′), 129.3 (C-3′,5′), 142.6 (C-6′), 20.9 ppm (CH_3). ^{19}F NMR (282 MHz, [D_6]acetone, 25 °C): δ −79.1 ppm (s, OTf). ESI-TOF MS: m/z 107 $[Ag]^+$ (17.3%), 202 $[L]^+$ (36.9%), 308 $[AgL]^+$ (100%), 509 $[AgL_2]^+$ (35.7%), 767 $[Ag_2L_2(OTf)]^+$ (2.6%). Elem anal. calcd (%) for $C_{11}H_{11}AgF_3N_5O_3S$ (458.2): C, 28.84; H, 2.42; N, 15.3. Found: C, 28.68; H, 2.38; N, 14.98.

Synthesis of $[Ag_3(Phdat)_2(OH_2)(acetone)_2(BF_4)_3]_n$, 7. To a solution of Phdat (20.6 mg, 0.11 mmol) in 3 mL of acetone was added solid $AgBF_4$ (41.6 mg, 0.21 mmol). After the solution was stirred, diethylether was allowed to diffuse over three days, and monocrystals of **7** as colorless plates appeared. They were filtered, washed with diethyl ether (2 × 1 mL), and dried with a nitrogen flow. IR (ATR): ν_{max}/cm^{-1} 3396 and 3327 (NH_2) and (OH_2), 1651 (O═CMe_2), 1581, 1556 and 1518 (C═N) and (C═C), 1061, 1042, 1020 and 978 ν(B−F). Elem anal. calcd (%) for $C_{24}H_{32}Ag_3B_3F_{12}N_{10}O_3$ (1092.6): C, 26.38; H, 2.95; N, 12.82. Found: C, 26.72; H, 2.84; N, 12.44.

Results and Discussion

Synthesis and Characterization. The different aminotriazine ligands were reacted with silver(I) salts in a metal-to-ligand ratio of 1:1 (see Scheme 2).

The products were obtained in high yields. According to the elemental analysis, the stoichiometry of the products **1**−**6** is AgLX (in the case of **1**, crystallization solvent is also included). After a finding of the NMR studies (see below), we crystallized a $AgBF_4$/Phdat mixture in a 2:1 ratio. Crystals of a new product, **7**, of stoichiometry $[Ag_3L_2(H_2O)(acetone)_2(BF_4)_3]$ were obtained from acetone/diethyl ether. The water of this compound must come from the silver salt. The IR spectra of the new compounds show bands corresponding to the ν(N−H), ν(C═N), or ν(C═C) vibrations. The presence of the counteranions was also corroborated from the vibration spectra (see the Experimental Section). In the case of the BF_4^- complexes **2** and **5**, the ν(B−F) band is split, a fact that indicates the existence of some kind of interaction involving the anion that decreases the T_d symmetry. In the case of **7**, four bands are observed in the ν(B−F) region around 1000 cm^{-1}.

We registered the mass spectra for complexes **1**−**6** (MALDI-TOF for **1**−**4** or ESI-TOF for **5** and **6**, see the Experimental Section for detailed data). For all derivatives, peaks corresponding to the fragments $[AgL]^+$ and $[AgL_2]^+$ were observed. The fragment $[Ag_2L_2]^+$ was also observed for all complexes except for those containing triflate groups where the fragments $[AgL(OTf)]^+$ (**3**) or $[Ag_2L_2(OTf)]^+$ (**6**) were detected. This is probably a consequence of the higher coordinating ability of this anion. When the ESI-TOF technique was used, peaks corresponding to $[Ag]^+$ and $[L]^+$ were also present.

X-Ray Structure Determination. The structures of complexes **2**, **3**, **5**, **6**, and **7** were determined by X-ray diffraction studies. The crystallographic data are given in Table 1. A selection of bond distances and angles are gathered in Table 2 for complexes **2** and **5** and in Table 3 for complexes **3**, **6**, and **7**. It was not possible to obtain crystals of the PF_6^- derivatives.

Complexes 2 and 5. Complexes [Ag(Phdat)](BF_4) and [Ag(Toldat)](BF_4) (**2** and **5**) were found to be isostructural, both crystallizing in the orthorhombic space group $I2_12_12_1$ with related unit cell dimensions. The structures of both compounds are very similar, and therefore only the phenyl compound is shown in the figures. A polymeric chain is formed, and this extends along the a axis and consists of {Ag(L)} fragments (Figure 1). Silver has an approximately linear coordination geometry [N1−Ag1−N1A angle of 179.5(3)° for **2** and 171.1(1)° for **5**] and is bonded to the triazine nitrogen atoms N^1 and N^5 (see Scheme 1 for atom numbering). The phenyl rings are practically perfectly flat (aplanarity <0.002 Å), but the triazine rings are remarkably aplanar and twisted, showing root mean square (rms) aplanarities of 0.056 Å (**2**) and 0.052 Å (**5**). In both complexes, the two rings of the ligand are not coplanar [interplanar angles of 39.9(4)° for **2** and 40.8(2)° for **5**]. Although not unprecedented in amino−triazine−metal systems,[20a,32] it is interesting to note that the silver centers are not in the same plane as the triazine rings: the distances to the plane are ±0.92(1) Å for **2** and ±0.845(5) Å for **5**. For a specific triazine ring, the two silver atoms bonded to it deviate in opposite directions. This deviation means that consecutive triazine rings are mutually inclined at angles of 53.8° in **2** and 59.6° in **5** and that the Ag−triazine chains have a helical character (see Figure 1a,b, where the sinusoidal character of the chain in two orthogonal planes can be observed). In fact, the analyzed crystals are chiral as a consequence of the fact that only P chains were found for both complexes (see Scheme S1, Supporting Information; the pitch, constituted by two silver centers and two ligands, is 12.02 Å in complex **2** and 11.68 Å in complex **5**). The triazine molecules exhibit a head-to-tail disposition.

(32) (a) Zhu, H.; Yu, Z.; You, X.; Hu, H.; Huang, X. *J. Chem. Cryst.* **1999**, *29*, 239–242. (b) Goodgame, D. M. L.; Hussain, I.; White, A. J. P.; Williams, D. J. *J. Chem. Soc., Dalton Trans.* **1999**, 2899–2900. (c) Chen, Ch.; Yeh, Ch.-W.; Chen, J.-D. *Polyhedron* **2006**, *25*, 1307–1312.

Table 1. Crystal Data and Structure Refinement for **2**·solv, **5**·solv, **3**, **6**, and **7**

	[Ag(Phdat)(BF$_4$)]$_n$·solv, **2**·solv	[Ag(Toldat)(BF$_4$)]$_n$·solv, **5**·solv	[Ag(Phdat)(OTf)]$_n$, **3**	[Ag(Toldat)(OTf)]$_n$, **6**	[Ag$_3$(Phdat)$_2$(H$_2$O)(Me$_2$CO)$_2$(BF$_4$)$_3$]$_n$, **7**
empirical formula	$C_9H_9AgBF_4N_5$	$C_{10}H_{11}AgBF_4N_5$	$C_{10}H_9AgF_3N_5O_3S$	$C_{11}H_{11}AgF_3N_5O_3S$	$C_{24}H_{32}Ag_3B_3F_{12}N_{10}O_3$
F_w[a]	381.89	395.91	444.15	458.18	1092.64
T (K)	180(2)	180(2)	173(2)	180(2)	100(2)
cryst size (mm^3)	0.34 × 0.22 × 0.18	0.53 × 0.37 × 0.31	0.63 × 0.28 × 0.19	0.44 × 0.08 × 0.04	0.55 × 0.32 × 0.03
cryst syst	orthorhombic	orthorhombic	monoclinic	monoclinic	monoclinic
space group	$I2_12_12_1$ (no. 24)	$I2_12_12_1$ (no. 24)	$P2_1/c$ (no. 14)	$P2_1/c$ (no. 14)	$C2/c$ (no. 15)
Z	4	4	8	8	4
a (Å)	12.017(5)	11.6841(11)	21.148(10)	12.552(5)	23.5390(6)
b (Å)	12.231(5)	11.9242(11)	7.283(4)	12.958(5)	13.8679(4)
c (Å)	12.402(5)	13.9294(11)	19.986(10)	19.320(7)	11.7781(3)
β (deg)	90	90	106.569(13)	90.167(7)	109.338(1)
V (Å^3)	1822.9(12)	1940.7(3)	2951(2)	3142(2)	3627.9(2)
ρ_{calcd} (g/cm^3)	1.392	1.355	2.000	1.937	2.000
μ_{calcd} (mm^{-1})	1.137	1.070	1.562	1.470	1.710
F(000)	744	776	1744	1808	2136
θ_{max} (deg)	28.24	27.49	27.04	25.00	29.95
total reflns measured	5887	7749	26580	26580	31036
ind reflns [R_{int}]	2192 [R_{int} = 0.077]	2229 [R_{int} = 0.026]	5690 [R_{int} = 0.087]	19421 [R_{int} = 0.149]	5254 [R_{int} = 0.029]
params refined, restraints	103, 0	108, 0	415, 128	435, 136	295, 10
final R1 [$I > 2\sigma(I)$]/all data[b]	0.047/0.057	0.023/0.025	0.087/0.115	0.072/0.151	0.031/0.075
final wR2 [$I > 2\sigma(I)$]/all data [b]	0.103/0.107	0.053/0.054	0.202/0.221	0.155/0.202	0.043/0.086
goodness of fit on F^2	0.991	1.059	1.047	1.003	1.120
solvent-accessible volume/cell [c]	654 (35.9%)	666 (34.3%)			
largest diff. peak and hole e·Å^{-3}	1.63 and −0.58	0.32 and −0.31	0.72 and −0.50	0.88 and −0.96	1.74 and −0.88

[a] The unknown solvent content of compounds **2**·solv and **5**·solv was SQUEEZED with program PLATON[31] prior to final refinement and is not contained in chemical formulae and quantities derived thereof (F_w, ρ_{calcd}, μ_{calcd}, and F(000)). [b] $R1 = \sum||F_0| - |F_c||/\sum|F_0|$ and $wR2 = \{\sum[w(F_0^2 - F_c^2)]/\sum[w(F_0^2)^2]\}^{1/2}$ [c] Solvent-accessible volume/cell: This is the volume (Å^3) of open space available to a sphere of radius 1.2 Å for the solvated compounds **2**·solv and **5**·solv.

Table 2. Selected Bond Distances and Angles for **2**·solv and **5**·solv

	[Ag(Phdat)(BF$_4$)]$_n$·solv, **2**·solv	[Ag(Toldat)(BF$_4$)]$_n$·solv, **5**·solv
Ag1−N1	2.142(4) (2×)	2.144(2) (2×)
N1−Ag−N1	179.5(3)	171.1(1)
Ag1−F	2.948(4) [F1] (2×)	2.923(2) [F1] (2×)
N1−C1	1.373(6)	1.365(3)
N1−C2	1.361(6)	1.339(2)
N2−C1	1.314(6)	1.338(3)
N3−C1	1.327(7)	1.316(3)
C2−C3	1.429(12)	1.461(6)
C3−C4	1.384(7)	1.394(3)
C4−C5	1.413(7)	1.385(4)
C5−C6	1.374(8)	1.369(4)
C6−C7		1.513(6)

The chains are packed parallel to the *ab* plane to give a warped sheet of chains linked through the BF_4^- groups (see Figure 2). These warped sheets are connected through interactions with the BF_4^- anions along the *c* axis. In this way, a sequence of planes ABAB... is obtained, with a mutual offset of the sheets by *a*/2 (Figure 2). This feature creates continuous channels along the *b* axis, and disordered solvent is included in these voids (in Figure 2, the solvent molecules have been removed). The average diameter of the channels is about 5 Å. Viewed along a {Ag(L)} chain, that is, parallel to the *a* axis, each chain is surrounded by six others in an elongated hexagonal disposition (see Figure S1, Supporting Information). The interactions that allow the formation of this network involve contacts between the fluorine atoms of the anions and different groups on the chains (see Table 4). Other examples have been described of chains that are linked through the anions via weak interactions[33,34] in silver compounds. In our case, there are hydrogen bonds[4] of the type NH···F and also CH···F bonds involving the aromatic ring, with the latter type being weaker.[33,35] There also exist Ag···F contacts.[9b,33,36] The Ag−F distances, 2.95 Å for **2** and 2.92 Å for **5**, are shorter than the sum of the van der Waals radii (3.19 Å).[37] Moreover, inside the chain there are short CH···Ag contacts[4d,38,39] (two per silver atom) with the ortho CH group of the aryl ring (see Table 4). The H···Ag and N···Ag distances also correspond to contacts between the NH_2 groups and the silver centers (see Table 4). These CH···Ag and NH_2···Ag contacts are present in all derivatives described in this paper and will not be detailed below (see Table 4 for the distances and angles)

Complex 3. This complex crystallizes in the monoclinic space group $P2_1/c$. A dimeric unit of formula [Ag$_2$(Phdat)$_2$(CF$_3$SO$_3$)$_2$] with two triflate bridges can be considered as the fundamental building block of this structure (see Figure 3). In this unit, each silver atom has a tetrahedral coordination geometry and is bonded to the two triflate bridges that exhibit a κ^2O,μ_2-*O* coordinative fashion and to one nitrogen atom of a triazine of the unit. Each silver center

(33) Wei, K.-J.; Ni, J.; Gao, J.; Liu, Y.; Liu, Q.-L. *Eur. J. Inorg. Chem.* **2007**, 3868–3880.

(34) (a) Fei, B.-L.; Sun, W.-Y.; Tang, W.-X. *J. Chem. Soc., Dalton Trans.* **2000**, 805–811. (b) Hsu, Y.-F.; Chen, J.-D. *Eur. J. Inorg. Chem.* **2004**, 1488–1493.

(35) (a) Grepioni, F.; Cojazzi, G.; Drapper, S. M.; Scully, N.; Braga, D. *Organometallics* **1998**, *17*, 296–307. (b) Manzano, B. R.; Jalón, F. A.; Ortiz, I. M.; Soriano, M. L.; Gómez de la Torre, F.; Elguero, J.; Maestro, M. A.; Mereiter, K.; Claridge, T. D. W. *Inorg. Chem.* **2008**, *47*, 413–428.

(36) (a) Zheng, Y.; Li, J.-R.; Du, M.; Zou, R.-Q.; Bu, X.-H. *Cryst. Growth Des.* **2005**, *5*, 215–222. (b) Halper, S. R.; Cohen, S. M. *Inorg. Chem.* **2005**, *44*, 486–488. (c) Hu, H.-L.; Yeh, C.-W.; Chen, J.-D. *Eur. J. Inorg. Chem.* **2004**, 4696–4701.

(37) Bondi, A. *J. Phys. Chem.* **1964**, *68*, 441–451.

(38) (a) Brookhart, M.; Green, M. L. H.; Parkin, G. *PNAS* **2007**, *104*, 6908–6914. (b) Crabtree, R. H. *Angew. Chem., Int. Ed.* **1993**, *32*, 789–805.

(39) Thakur, T. S.; Desiraju, G. R. *Chem. Commun.* **2006**, 552–554.

Table 3. Selected Bond Distances (Å) and Angles (deg) for **3**, **6**, and **7**

[Ag(Phdat)(OTf)]$_n$, **3**		[Ag(Toldat)(OTf)]$_n$, **6**		[Ag_3(Phdat)$_2$(H_2O)(Me_2CO)$_2$ (BF_4)$_3$]$_n$, **7**	
Ag1−N1	2.375(8)	Ag1−N1	2.297(8)	Ag1−N1	2.246(2)
Ag1−N3	2.298(8)	Ag1−N6	2.222(8)	Ag1−N3[a]	2.240(2)
Ag1−O2	2.413(11)	Ag1−O1	2.558(7)	Ag1−O1	2.439(2)
Ag1−O4	2.364(9)	Ag1−O4	2.494(7)	Ag1−F7	2.810(2)
Ag2−N6	2.327(8)	Ag2−N2	2.202(8)	Ag2−N2	2.193(2)
Ag2−N8	2.379(8)	Ag2−N8	2.225(8)	Ag2−O2	2.716(2)
Ag2−O1	2.445(9)	Ag2−O2	2.573(7)		
Ag2−O5	2.423(10)	Ag2−O4	2.578(7)		
N1−Ag1−N3	109.9(3)	N1−Ag1−N6	135.2(3)	N1−Ag1−N3[a]	132.49(8)
N1−Ag1−O2	116.6(5)	N1−Ag1−O1	91.0(3)	N1−Ag1−O1	117.68(6)
N1−Ag1−O4	95.9(3)	N1−Ag1−O4	81.7(3)	N3[a]−Ag1−O1	109.49(6)
N3−Ag1−O2	115.9(5)	N6−Ag1−O1	98.6(3)	O1−Ag1−F1	85.87(7)
N3−Ag1−O4	133.2(4)	N6−Ag1−O4	137.8(3)	N1−Ag1−F1	83.75(8)
O4−Ag1−O2	83.2(5)	O1−Ag1−O4	100.4(2)	N2[b]−Ag2−N2	180.0
N6−Ag2−N8	109.9(3)	N2−Ag2−N8	146.5(3)	O2−Ag2−O2	180.0
N6−Ag2−O1	127.5(4)	N2−Ag2−O2	101.7(3)	N2−Ag2−O2	81.49(9)
N6−Ag2−O5	118.0(5)	N2−Ag2−O4	104.9(3)		
N8−Ag2−O1	94.5(3)	N8−Ag2−O2	92.4(3)		
N8−Ag2−O5	116.9(5)	N8−Ag2−O4	97.7(3)		
O1−Ag2−O5	87.3(4)	O2−Ag2−O4	111.6(2)		

[a] $x, -y, z + 1/2$. [b] $-x + 1/2, -y + 1/2, -z + 1$.

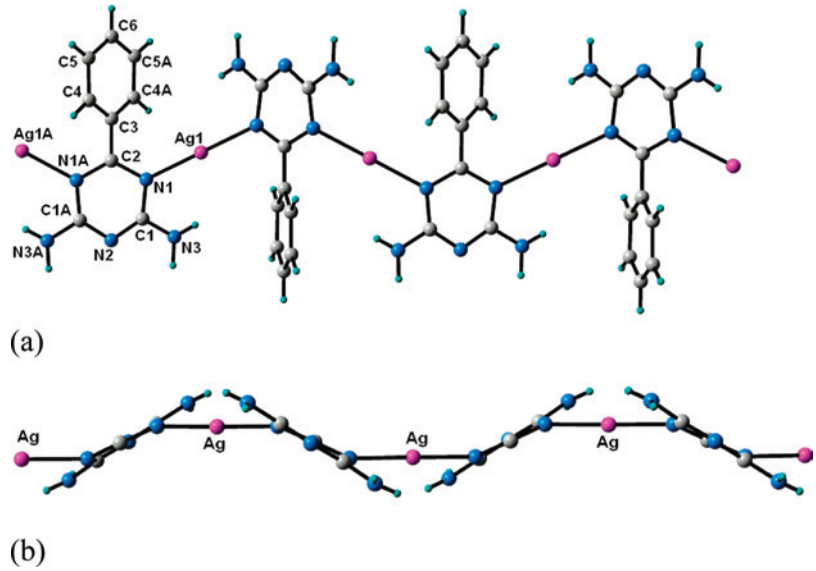

Figure 1. The polymeric chain of complex **2** that extends along the *a* axis: (a) view along the *c* axis and atom numbering; (b) view along the *b* axis with phenyl groups omitted for clarity.

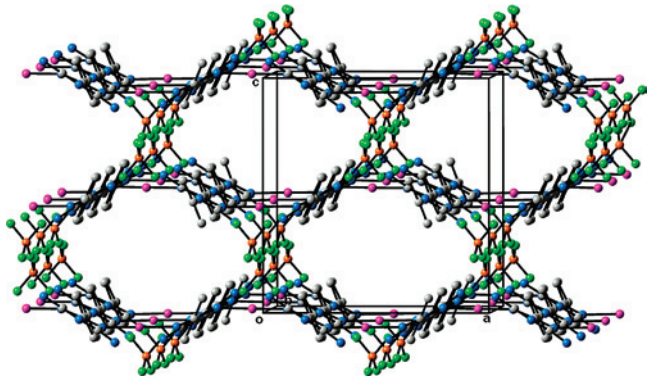

Figure 2. Complex **2**. Ball and stick view of the channels that extend along the *b* axis formed with three sheets. The {Ag(L)} chains shown in Figure 1 are connected through interactions with the BF_4 anions. Pink = Ag; blue = N; grey = C; orange = B; green = F; pale blue = H.

is also bonded to a triazine ring of another unit. The Ag−Ag distance is 5.68 Å. In addition, one nitrogen atom of each triazine ring is bonded to silver atoms of other units. Consequently, each dimeric unit is bonded to another four units that are rotated by 180° with respect to the former around the crystallographic *b* axis (see Figure 4). In this way, a sheet extending along the *ab* plane is formed. The O−Ag−O angles (83−87°) are considerably smaller than the N−Ag−N angles (109.9°). The nitrogen atoms used to coordinate to the silver center are, as in the previous complexes, N^1 and N^5 of the triazine rings. The thickness of the sheets, measured as the distance between the two limiting and parallel planes passing through the *para*-H of the phenyl rings, is 8.93 Å.

It can be clearly seen in Figure 4a that the two rings of a specific triazine ligand are not located in the same plane, and the corresponding interplanar angles are 45.1° (phenyl-triazine 1 with N1) or 43.2° (phenyl-triazine 2 with N6). As in the previous complexes, the silver atoms are not in the same plane as the triazine rings, the distances between Ag and these planes being ±0.64 and ±0.93 Å. In contrast to **2**

Table 4. Distances (Å) and Angles (deg) for Noncovalent Interactions in Complexes **2**, **3**, **5**, **6**, and **7**

	hydrogen bonds in the ligands								
	NH···F		CH···F			CH···Ag		NH···Ag	
compd	N3−(H)···F	NHF	C4−(H)···F1	CHF	Ag1···F1	C−(H)···Ag	CHAg	N−(H)···Ag	NHAg
2	2.96(1) [F1]	119	3.28(1)	140	2.948(4) (2×)	3.181(6) [C4,Ag1]	96	3.246(5) [N3,Ag1]	114
	3.00(1) [F1]	146							
	2.96(2) [F2]	166							
	2.97(2) [F3]	171							
5	3.081(3) [F1]	148	3.319(3)	137	2.923(2) (2×)	3.099(2) [C4,Ag1]	95	3.281(2) [N3,Ag1]	114
	3.196(4) [F2]	138							
	3.05(2) [F3]	154							
	3.18(2) [F3]	148							

	NH···O (intra[a])		NH···O (inter[b])		CH···Ag		NH···Ag	
	N−(H)···O	NHO	N−(H)···O	NHO	C−(H)···Ag	CHAg	N−(H)···Ag	NHAg
3	2.99(2) [N4,O4]	166	3.00(2) [N4,O3]	158	2.94(1) [C5,Ag1]	96	3.55(1) [N4,Ag1]	120
	3.10(2) [N5,O3]	131	3.00(1) [N5,N2]	159	3.06(1) [C9,Ag1]	90	3.54(1) [N5,Ag1]	113
	2.93(2) [N9,O6]	136	3.02(1) [N9,N7]	157	2.94(1) [C14,Ag2]	91	3.51(1) [N9,Ag2]	116
	3.01(2) [N10,O1]	152	3.36(2) [N10,O6]	142	3.11(1) [C18,Ag2]	93	3.62(1) [N10,Ag2]	115
6	3.10(1) [N4,O1]	164	2.90(1) [N5,N7]	158	3.36(1) [C5,Ag1]	91	3.18(1) [N9,Ag1]	118
	3.24(1) [N4,O4]	174	2.99(1) [N9,N3]	159	3.14(1) [C15,Ag2]	88	3.13(1) [N5,Ag2]	117
	3.14(1) [N5,O2]	168						
	3.01(1) [N9,O1]	165						
	3.04(1) [N10,O2]	167						
	2.88(1) [N10,O5]	159						

	NH···F (intra[a])		AH···B (inter[b])		C−(H)···Ag	CHAg	N−(H)···Ag	NHAg
7	2.874(6) [N4,F5]	130	2.728(3) [O1,F4]	143	3.193(3) [C5,Ag1]	91	3.359(3) [N4,Ag1]	110
			2.993(4) [N5,O2]	146	3.011(3) [C9,Ag2]	95	3.268(3) [N4,Ag1]	110
			3.125(4) [N5,F1]	138			3.302(2) [N5,Ag2]	117
			3.061(5) [N5,F3]	155				
			3.041(2) [N4,F4]	166				
			3.199(7) [N4,F6]	124				
			3.435(3) [N4,F7]	177				

[a] Intra refers to intralayer in the case of **3** and to intraladder in the cases of **6** and **7**. [b] Inter refers to interlayer in the case of **3** and to intraladder in the cases of **6** and **7**.

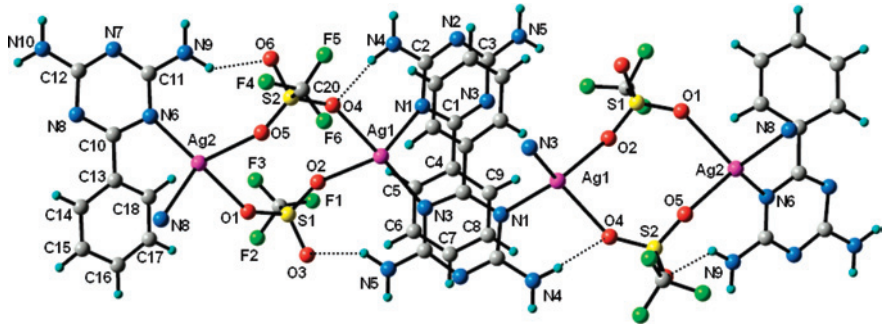

Figure 3. Structural diagram of compound **3** including intralayer hydrogen bonds.

and **5**, the triazine rings are practically planar in complex **3** (aplanarity < 0.02 Å).

As shown in Figures 3 and 4, in the structure there is a noticeable motive for assembly between the elemental building blocks—namely, triazine−phenyl $\pi-\pi$ stacking.[5] The respective electron-poor and electron-rich character of these aromatic rings reinforces the bonding in the lamellar structure. This stacking extends along the crystallographic *b* axis and leads to the formation of columns of alternating electron-poor and electron-rich aromatic rings (the columns are indicated by arrows in Figure 4c). Columnar stacking between aromatics and triazine rings has also been described by Fujita et al.[15c,d] The intercentroid ring distances display alternate values of 3.78 and 3.52 Å and the centroid−plane distances are in the range 3.36−3.40 Å, with an angle between planes of 3.3−3.8° and a slipping angle of 17.5−25.9°. There are also intralayer N−H···O hydrogen bonds between NH_2 and the triflate groups (see Table 4 and Figure 3). These bonds involve the two amino hydrogens that are oriented toward the inside of the sheet and free as well as Ag-coordinated oxygen atoms of the counteranion.

As can be seen from Figure 5, the asymmetric unit has an arrangement of four ADAD centers constituted by the uncoordinated oxygen atom of a triflate, an amino group, the triazine N^3 atom, and the second amino group. In the adjacent sheet, there exist the complementary DADA groups related by inversion, and in this way, sets of four hydrogen bonds are formed that connect the 2D networks perpendicular to (001) to form a three-dimensional superstructure (see Table 4 for the hydrogen-bonding distances).

Complex 6. This complex crystallizes in the space group $P2_1/n$. It is remarkable that **6** differs from **5** only in an

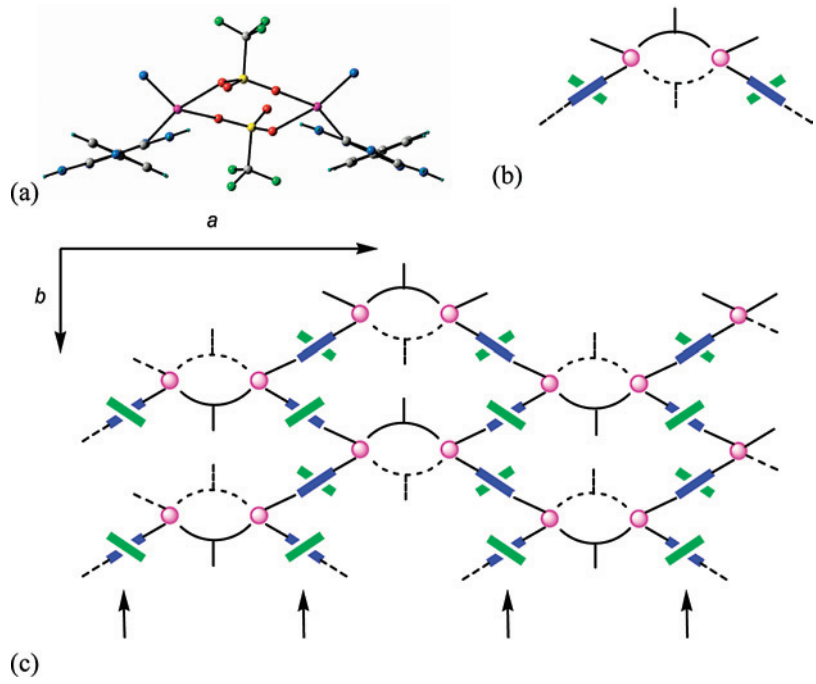

Figure 4. (a) Schematic view of the building unit of **3**. (b) Schematic representation of the unit. A continuous or a dotted line represents a triflate bridge that is in front of or behind the projection plane. A blue rectangle represents the triazine ring and a green rectangle the phenyl ring. (c) 2D network of one sheet. The arrows represent the columns in which $\pi-\pi$ stacking is present.

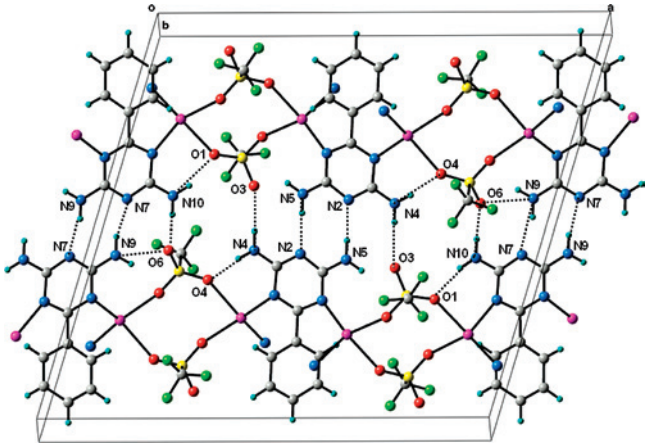

Figure 5. Crystal structure of **3** with unit cell viewed along the *b* axis. Intra- and interlayer NH···N and NH···O hydrogen bonds are marked as dotted lines.

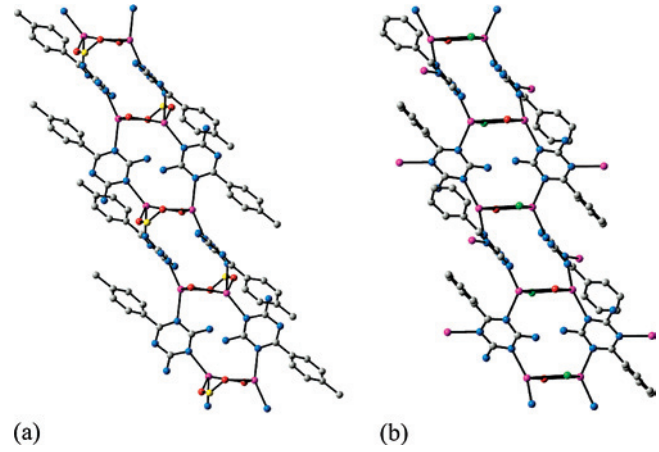

Figure 6. (a) Ladderlike polymer of complex **6** that extends along the *a* axis. (b) The same for complex **7** along the *c* axis. The H atoms and those atoms of the bridging groups that do not participate in the bridge have been omitted for clarity.

additional methyl group, but the structure is completely different. The structure can be considered as consisting of ladderlike polymers that extend along the *a* axis and are mutually connected through hydrogen bonds to build a 3D supramolecular architecture. The ladders have several special characteristics that make them very unusual (see Figures 6a and 7). In principle, this structure may be compared with the structure of $NbOCl_3$[40] in the sense that the rungs are constituted by a double bridge. In both structures, the nodes are the metallic centers, and in the niobium derivative, the bridges are the chlorine atoms, whereas in complex **6**, the two triflate groups form an asymmetric bridge. In fact, one triflate is coordinated in a κ^2O,μ_2-*O* fashion, and in the other, the same oxygen atom is bonded to the two silver centers (κ^1O,μ_2-O). The four silver atoms define a parallelogram, and the sides of the ladder are occupied by triazine ligands situated in parallel planes and bonded this time through the N^1 and N^3 atoms and with a head-to-tail disposition. However, in contrast to the situation usually found in ladder structures, the two ligands are not eclipsed but are clearly displaced. In the middle of the resulting Ag_4 unit, there is an inversion center. This parallelogram is fused with another one in which the triazine ligands have a different orientation. The dihedral angle formed by two consecutive triazine rings is 70.3°. In this way, the fused Ag_4 units alternate the orientation of the triazines along the polymer. As in the previous complexes, the triazine and aryl (tolyl) rings are not coplanar (dihedral angles between 37 and 42°). Likewise, the silver centers are not in the triazine planes showing

(40) (a) Sands, D. E.; Zalkin, A.; Elson, R. E. *Acta Crystallogr.* **1959**, *12*, 21–23. (b) Ströbele, M.; Meyer, H.-J. *Z. Anorg. Allg. Chem.* **2002**, *628*, 488–491.

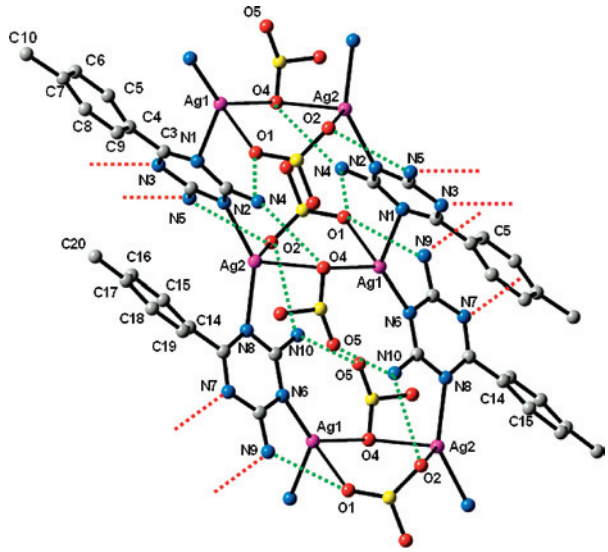

Figure 7. Complex **6**. Two fused units showing the intramolecular (in green) and the intermolecular (in red) hydrogen bonds. H atoms and CF_3 groups omitted for clarity. Yellow = S.

comparatively large deviations (distances to triazine planes vary from 0.71 to 1.48 Å). The two independent silver atoms exhibit distorted tetrahedral coordination geometries (see Table 4 for the distances and angles). Like in **3**, the O−Ag−O angles are smaller than the N−Ag−N angles, with both of these angles larger than those found in the phenyl derivative. In fact, one N−Ag−N angle has a value of 146.4°.

Each Ag_4 unit has four amino groups, that is, eight hydrogen donors to form hydrogen bonds, and as acceptors, there are the oxygen atoms of the triflate anions and triazine N^5 atoms. Inside this parallelogram, six hydrogen bonds are formed involving the triflate groups (see Figure 7). Interestingly, one hydrogen donor and the N^5 atom of each ligand are oriented outside the unit and form a double hydrogen bond with another chain. In this way, the chain is hydrogen-bonded to two neighboring chains in the [011] direction. The subsequent unit within the chain, displaced relative to the preceding by *a*/2, has the same hydrogen-bonding system but adopts a (010) mirror related orientation. Therefore, it links with two neighboring chains in the [01$\bar{1}$] direction. As a result, a 3D supramolecular structure is formed (Figure 8a). The existence of this hydrogen-bonded net means that all of the hydrogen-bond donors and acceptors of the triazine ring are used in the formation of hydrogen bonds. The tolyl groups are situated outside the chains and define hydrophobic regions that are parallel to the *ab* plane. The OTf groups are oriented with their CF_3 groups tail-to-tail with mutual F···F contacts approximately parallel to the *b* axis.[41] The F···F contact distances are about 2.9 Å and should be considered as virtual because both CF_3 groups apparently suffer from orientation disorder, as indicated by their large anisotropic displacement parameters.

As stated above, the structure of complex **6** can be considered as a very unusual type of ladderlike structure. Although other examples of double-bridged rungs are known,[42] it is not common for these to be asymmetric in nature. Even though a silver ladder structure in which octagons and rhombuses alternate along the chain have been described,[43] in our case, the offset disposition of the sides and the alternating orientation of ligands in these sides are extremely uncommon. These two facts give to the polymer a more three-dimensional nature, and this could also be considered as a tubular chain.

Complex 7. This compound crystallizes in the monoclinic space group *C*2/*c*. Its composition may be given as $Ag_2(Phdat)_2(H_2O)(BF_4)_2 \cdot Ag((CH_3)_2CO)_2(BF_4)$. The compound is built up from a Ag1 ion in triangular planar coordination by two triazine nitrogen atoms and the oxygen atom of a water molecule (Figure 9). The triangular-planar coordination of Ag1 is supplemented by two F atoms from two inequivalent BF_4 tetrahedra to form a very distorted trigonal bipyramidal coordination figure $Ag(N_2OF_2)$. The Ag−F distances are shorter than the sum of the van der Waals radii (Table 3), and cases have been described of interactions or bonds with similar values.[44] The second Ag atom of the compound, Ag2, is in a special position with point symmetry C_i and has a square-planar coordination by two triazine nitrogen atoms N^5 and two weakly bonded oxygen atoms[45] of acetone molecules. The Phdat ligand is in a general position and consists of two essentially flat six rings (rms aplanarities of 0.035 Å for the triazine ring and of 0.018 Å for the phenyl ring) with a dihedral ring−ring inclination of 47.8(9)°. It is bonded to two Ag1 via N^1 and N^3 and to one Ag2 via N^5. The silver centers are outside the triazine plane (distances of ±0.874(1) Å for Ag1 and ±0.4700(2) for Ag2). There are two independent BF_4 tetrahedra, of which that of B1 is in a general position and terminally bonded to Ag1, whereas that of B2 together with its F7 atom (weakly bonded to two Ag1) is located on a 2-fold axis, which implies that the remaining three F atoms of B2 are disordered, being distributed over three half-occupied positions, F5, F7, and F8. The water molecule H_2O1 is located on a 2-fold axis and bridges two Ag1's (Ag−O−Ag = 110.7(7)°). The acetone molecule as the last constituent is in general position and terminally bonded to one Ag2 with an angle C32═O2−Ag2 = 147°.

The Ag1 atoms and the triazine ligands define a ladderlike polymer constituted by fused Ag_4 units (extended along the

(41) (a) Vangala, V. R.; Nangia, A.; Lynch, V. M. *Chem. Commun.* **2002**, 1304–1305. (b) Metrangolo, P.; Neukirch, H.; Pilati, T.; Resnati, G. *Acc. Chem. Res.* **2005**, *38*, 386–395.

(42) (a) Hou, H.; Xie, L.; Li, G.; Ge, T.; Fan, Y.; Zhu, Y. *New. J. Chem.* **2004**, *28*, 191–199. (b) Zhang, G.; Yang, G.; Shi, M. *J. Cryst. Growth Des.* **2006**, *6*, 1897–1902.

(43) Zhong, J. C.; Munakata, M.; Maekawa, M.; Kuroda-Sowa, T.; Suenaga, Y.; Konaka, H. *Inorg. Chim. Acta* **2003**, *342*, 202–208.

(44) (a) Camalli, M.; Caruso, F. *Inorg. Chim. Acta* **1987**, *127*, 209–213. (b) Carlucci, L.; Ciani, G.; Proserpio, D. M.; Sironi, A. *J. Am. Chem. Soc.* **1995**, *117*, 4562–4569. (c) Bertelli, M.; Carlucci, L.; Ciani, G.; Proserpio, D. M.; Sironi, A. *J. Mater. Chem.* **1997**, *7*, 1271–1276. (d) Haftbaradaran, F.; Draper, N. D.; Leznoff, D. B.; Williams, V. E. *Dalton Trans.* **2003**, 2105–2106.

(45) (a) Edema, J. J. H.; Stock, H. T.; Buter, J.; Kellogg, R. M.; Smeets, W. J. J.; Spek, A. L.; Bolhuis, F. *Angew. Chem., Int. Ed. Engl.* **1993**, *32*, 436–439. (b) Bowmaker, G. A.; Effendy; Marfuah, S.; Skelton, B. W.; White, A. H. *Inorg. Chim. Acta* **2005**, *358*, 4371–4388. (c) Powell, J.; Horvath, M. J.; Lough, A.; Phillips, A.; Brunet, J. *Dalton Trans* **1998**, 637–645. (d) Doppelt, P.; Baum, T. H.; Ricard, L. *Inorg. Chem.* **1996**, *35*, 1286–1291. (e) Chen, X.-D.; Mak, T. W. *J. Mol. Struct.* **2005**, *748*, 183–188.

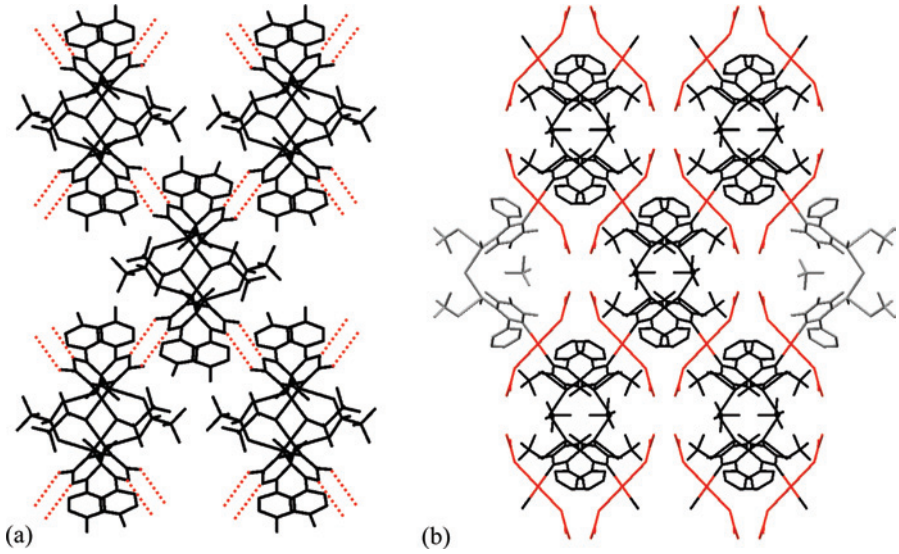

Figure 8. (a) View down the *a* axis of five chains connected through pairs of hydrogen bonds for complex **6**. (b) View down the *c* axis of five chains (in black) connected through "Ag(acetone)$_2$" fragments (in red) for complex **7**. H atoms omitted for clarity.

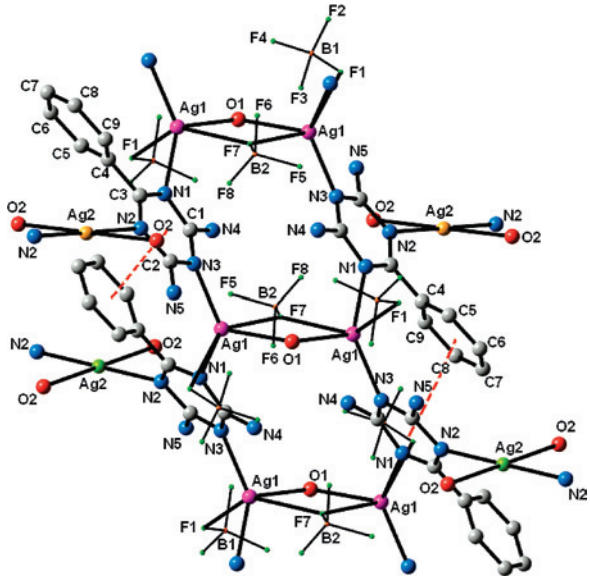

Figure 9. Two fused units of complex **7**. The silver centers of the ladder are in pink. The silver atoms in green or yellow form the sheets on different planes (see text). Only the hydrogen bonds inside the ladder are indicated (green). In red are the $\pi-\pi$ interactions.

c axis) very similar to that of **6**. The nodes are the silver centers, and the rungs are also constituted by a double and asymmetric bridge. In this case, instead of the triflate anions, it consists of the water molecule and the B(2)F_4^- group. The triazine ligands form the sides of the ladder, and they are situated in a very similar way to that of **6**. As in **6**, in complex **7**, the fused Ag_4 units also alternate the orientation of the triazines along the polymer (see Figure 6b and compare with Figure 6a). The dihedral angle formed by two consecutive triazine rings is 53.2°.

A differentiated fact found in **7** that was not observed in **6** is the existence of $\pi-\pi$ stacking between triazine and phenyl rings of consecutive Ag_4 units (see Figure 9, red lines). The angle formed between the two planes is 5.3°; the centroid−centroid distance is 3.65 Å; the centroid−plane distances are 3.47 and 3.40 Å, and the slipping angles are 18 and 21°. In this complex, there are also short distances between F atoms of the B(2)F_4^- group and the triazine ring (F-plane distances of 2.9−3.2 Å) that are indicative of anion$-\pi$ interaction. This type of interaction is receiving increasing attention, and it has been found involving triazine rings.[35b,46]

In this compound, intraladder hydrogen bonds involving NH_2 groups and the BF_4^- situated inside the ladder are observed. Outside the ladder, there are also these kinds of bonds with the participation of NH_2 and BF_4^- groups and also the oxygen atoms of water and acetone molecules.

One unit of the ladder is connected to the other two ladders to form a sheet [along the plane (220)], and the following unit is also connected in the same way but to form a sheet in the plane ($2\bar{2}0$). In this way, the 3D dimensional structure is formed. This is completely similar to that found in **6**, but perhaps the most intriguing thing is that the role played by the hydrogen bonds in **6** to build the superstructure is played here by [Ag(acetone)$_2$] units that are bonded to two triazine ligands from two different chains (see Figure 8b). In this way, complex **7** can be considered as a MOF derivative. It is observed that the methyl groups of the acetone ligands are oriented toward the same region of the space (hydrophobic effect), and the BF_4^- groups occupy holes formed in the structure.

From the topological point of view and considering that the bridges and the [Ag(acetone)$_2$] fragments are not nodes, the three-dimensional framework of **7** is a (3,3)-connected net, comprised of silver centers and ligands with the Schäfli

(46) (a) Mascal, M.; Armstrong, A.; Bartberger, M. D. *J. Am. Chem. Soc.* **2002**, *124*, 6274–6276. (b) Demeshko, S.; Dechert, S.; Meyer, F. *J. Am. Chem. Soc.* **2004**, *126*, 4508–4509. (c) Frontera, A.; Saczewski, F.; Gdaniec, M.; Dziemidowicz-Borys, E.; Kurland, A.; Deyà, P. M.; Quiñonero, D.; Garau, C. *Chem.—Eur. J.* **2005**, *11*, 6560–6567, and references therein. (d) Schottel, B. L.; Chifotides, H. T.; Shatruck, M.; Chouai, A.; Pérez, L. M.; Bacsa, J.; Dunbar, K. R. *J. Am. Chem. Soc.* **2006**, *128*, 5895–5912. (e) Schottel, B. L.; Chifotides, H. T.; Dunbar, K. R. *Chem. Soc. Rev.* **2008**, *37*, 68–83.

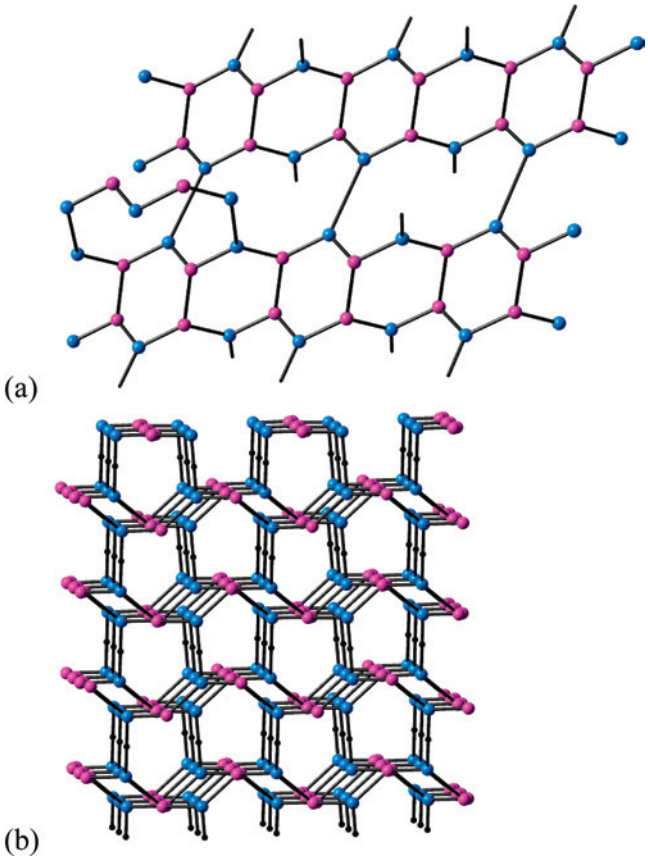

Figure 10. Topological representation of **7**. (a) Partial view to emphasize the nodes in the cycles. (b) View down the *a* axis. Blue and pink circles represent the ligands and silver centers of the ladders, respectively. The small black circles represent the [Ag(acetone)$_2$] fragments that connect the ladders.

symbol of $(6^2.10)(6.10^2)$.[47] In Figure 10, two schematic representations of the network where the ladders run horizontally are gathered. Figure 10a represents a section of the framework, and it is intended to reflect the number of nodes in the cycles.

Comparative Analysis of the Structures of 2, 3, 5, 6, and 7. On comparing the self-assembled supramolecular architectures of the new compounds, several facts can be clearly established. In all cases, the silver center is not in the same plane as the coordinating triazine ring (distances up to ±1.48 Å), and the triazine rings are not coplanar with the phenyl or tolyl groups (dihedral angles in the range of 37−48°). The latter situation is in contrast to that found in the free ligand Phdat[17] where the interplanar angles for the two independent molecules are 6.0 and 9.3° (the X-ray structure of Toldat has not been described). In this sense, we can state that coordination to the silver center disturbs the conformation of the triazine ligands, at least in the case of Phdat. In all derivatives, weak NH···Ag and CH···Ag interactions have been detected. In the derivatives with a Ag/L ratio of 1, one nitrogen atom of the triazine ring is not coordinated to the silver centers. In derivatives **2**, **3**, and **5**, it is N^3, while for complex **6**, it is N^5. When comparing these four complexes, it is deduced that the type of anion present has a dramatic influence on the silver coordination number and also on the final supramolecule formed. This effect seems to be mainly related to the coordinating ability of the anion. Several examples of anion control in silver coordination polymers have been described.[1f] In some cases, a difference in the anion coordinating behavior is observed[26,36c,48−50] although in others the differences are due to other factors,[8,27,33,51] including, for example, their size[51] or their shape.[4c] In our case, the coordination of the oxygen atoms of the triflate group induces the formation of double triflate bridges. On the other hand, the type of aryl group present on the triazine ligand may have an influence on the network topology. Complexes **2** and **5**, both of which contain the BF_4 anion, have identical structures. It seems that the methyl groups of the tolyl rings are oriented toward regions of space whose occupation does not have significant consequences on the final architecture. The difference between a phenyl and a tolyl group is small but sometimes gives rise to very important changes in behavior.[19b] In fact, in the triflate complexes, the presence of the methyl group on the aryl ring leads to a dramatic change in the structure. In the phenyl derivative, sheets exhibiting columns with $\pi-\pi$ stacking and connected through hydrogen bonds are formed, but the tolyl complex gives rise to a tubular chain in which the stacking is not observed, but the system adopts a disposition where an extensive net of hydrogen bonds is established. In fact, a common feature of the two derivatives is the presence of a large number of hydrogen bonds involving the triazine and triflate groups in such a way that all of the hydrogen donor or acceptor groups from the triazine ring are involved. Some of these bonds are internal, but others are intermolecular and increase the dimensionality of the derivatives from 2D to 3D (**3**) or 1D to 3D (**6**). It can be stated that, for the OTf complexes, the double hydrogen bond N−H···N/N···H−N present in the free triazine ligands is maintained (amplified to a quadruple bond in the case of **3**). This hydrogen bond is completely broken in the BF_4 derivatives **2** and **5**, and weaker noncovalent interactions involving the counteranion are present, thus increasing the dimensionality from 1D to 3D. All of theses structures show that, besides the covalent bonds between the silver centers and the ligands, the architecture is largely influenced by the noncovalent interactions.

Perhaps the most striking fact comes from the comparison of the structures of compounds **6** and **7**. Although they differ

(47) (a) Wells, A. F. *Further Studies of Three-Dimensional Nets*, 1st ed.; American Crystallographic Association Press: Buffalo, NY, 1979; Monograph Number 8. (b) Bucknum, M. J. *CPS:physchem/0202007*, 2002, 1−25. (c) Bucknum, M. J. *CPS: physchem/0202006*, 2002, 1−40. (d) Carlucci, L.; Ciani, G.; Proserpio, D. M.; Rizzato, S. *J. Solid State Chem.* **2000**, *152*, 211–220.

(48) Seward, C.; Chan, J.; Song, D.; Wang, S. *Inorg. Chem.* **2003**, *42*, 1112–1120.

(49) Wu, H.-P.; Janiak, C.; Rheinwald, G.; Lang, H. *J. Chem. Soc., Dalton Trans.* **1999**, 183–190.

(50) (a) Withersby, M. A.; Blake, A. J.; Champness, N. R.; Hubberstey, P.; Li, W.-S.; Schröder, M. *Angew. Chem., Int. Ed.* **1997**, *36*, 2327–2329. (b) Hu, H.-L.; Yeh, C.-W.; Chen, J.-D. *Eur. J. Inorg. Chem.* **2004**, 4696–4701. (c) Chi, Y.-N.; Huang, K.-L.; Cui, F.-Y.; Xu, Y.-Q.; Hu, C. W. *Inorg. Chem.* **2006**, *45*, 10605–10612.

(51) Long, D.-L.; Hill, R. J.; Blake, A. J.; Champness, N. R.; Hubberstey, P.; Wilson, C.; Schröder, M. *Chem.−Eur. J.* **2005**, *11*, 1384–1391. (a) Kim, H.-J.; Zin, W.-C.; Lee, M. *J. Am. Chem. Soc.* **2004**, *126*, 7009–7014.

in the stoichiometry, counteranions, and triazine substituents, their structures show an amazing degree of resemblance. They exhibit extremely similar ladderlike structures. It is also very noteworthy that the connection between these chains to form a 3D structure that consists of similar crossed sheets is effected in complex **6** by hydrogen bonds and in **7** by silver centers. That is to say, the silver center and the double hydrogen bond interchange their roles. As for differences, in **7** there exist triazine−phenyl $\pi-\pi$ stacking and anion$-\pi$ (triazine$-BF_4$) interactions.

Powder X-Ray Diffraction and Thermal Analysis. For compounds **2**, **3**, and **6**, it was verified by powder X-ray diffraction that the monocrystals were representative of the bulk material (it was supposed that **5** was similar to **2**). For **7**, the repeated formation of the same derivative was verified because the same structure was obtained from three monocrystals from three different preparations (only the third monocrystal was good enough to get data of quality).

A TGA and DTA analysis was performed for **2** and **7**. In the case of **2**, the presence of THF, acetone, and water was detected from ^{1}H NMR spectra. When a freshly prepared sample was heated (Figure S2, Supporting Information), an initial mass loss of 8.3% was detected up to ca. 155 °C. Within it, a change in the slope was observed, and two mass variations of approximately 3.6 and 4.6% can be considered. The first could correspond to the loss of acetone and THF and the second to a mole of H_2O per mole of complex. At the same time, an endothermic peak appeared centered at 156 °C. When the sample was not freshly prepared (Figure S3, Supporting Information), this initial loss was 3.7%, indicating a previous and partial loss of solvents on storage. In both samples, an exothermic peak was also observed at 196 °C, while the weight remained constant. At approximately 260 °C, it started a second mass loss, and an endothermic peak was also observed with two maxima at 319 and 330 °C. When the sample was recovered, it was a spongy black material, a fact that reflects the decomposition of the product. In order to get further information about the exothermic peak, two samples of **2** were heated in the ATD-TG apparatus, one up to 170 °C (**2**-170) and the other up to 220 °C (**2**-220), and a powder diffractogram was recorded for both. The sample **2**-170 is amorphous (Figure S4, Supporting Information), while **2**-220 is crystalline (Figure S5, Supporting Information) with a pattern different from that of the nonheated sample. Consequently, the loss of the solvents of the channels leads initially to an amorphous sample which, on heating, is transformed into a crystalline structure probably more compact than the initial one, and the peak observed at 196 °C corresponds to this transformation.

In the case of **7**, a very slow mass reduction of 3.5% up to approximately 280 °C accompanied by a weak endothermic peak was observed (Figure S6, Supporting Information). This must correspond to the loss of acetone and water. The value of 3.5% (smaller than the mass percentage of these solvents in the formulas, 12.3%) indicates that the solvents have been partially lost at room temperature. At ca. 280 °C, a sharp mass variation starts, and at the same time, an endothermic peak with several maxima between 300 and 350 °C appears, reflecting the decomposition of the material (a black solid is obtained). It is interesting to note that in complex **7** where the channels are not present the exothermic peak found in **2** does not appear.

NMR Characterization in Solution. It is well-known that silver complexes with nitrogenated ligands exhibit in solution a dynamic behavior involving interconversion between different species.[10,13,27,48] When low-temperature NMR spectra are recorded, although changes in chemical shifts are observed, the interconversion process is not usually slowed down enough to detect specific species.[27,48] A case has been described of a silver complex where a ring-spinning process is frozen out at low temperatures in solution due to a CH$\cdots\pi$ interaction.[52] We were interested in studying the behavior of our derivatives in solution, and room-temperature and low-temperature NMR spectra were recorded. Fortunately, we were able to detect a new species in solution.

In the room-temperature ^{1}H NMR spectra of all derivatives, the R groups in the 6 position of the triazine ring appear to be symmetric. A single broad resonance assigned to the NH_2 groups is also observed. With the exception of the ortho protons of the aromatic rings, deshielding of the signals is observed with respect to the free ligands, a fact due to the donation of electron density to the metal center. The shift is clearly higher for the amine resonances ($\Delta\delta = 0.4-1.0$). In the corresponding ^{19}F NMR spectra, the counteranion resonances are sharp signals. The ^{13}C {^{1}H} NMR spectra were only recorded for the more soluble derivatives (see the Experimental Section) and also reflect the presence of symmetric ligands. Although these facts may also be due to the presence of highly symmetric species, we propose that an exchange process exists in solution.

The ^{1}H NMR spectra of all complexes at low temperatures (−80 °C, acetone-d_6) were also recorded. As in the free triazines, the broad resonance assigned to the NH_2 groups is split into two signals at −80 °C. This indicates a more restricted rotation of the triazine$-NH_2$ bond at low temperatures. In addition, the chemical shift (averaged) of these resonances increases. Both of these facts could be related to the existence of DA/AD hydrogen-bond pairs between pairs of ligands in solution. As far as the resonances of the R group of the triazine ring are concerned, a slight broadening of some signals is observed in all cases. For instance, a broadening of the ortho resonance of complex **1** was observed at low temperatures. These observations indicate that the dynamic processes are also operating at −80 °C in acetone.

The distinct behavior of complexes **2** and **3** is noticeable. Besides the splitting of the NH_2 resonances and the presence of several signals similar to those found at room temperature, a set of five new resonances (one overlapped) of equal intensity are observed at −80 °C (see Figure 11). The studies described below were carried out on complex **2** because the resonances at low temperatures were sharper. A ^{1}H$-^1$H correlation spectroscopy spectrum demonstrated that the new signals are coupled and belong to a single phenyl group (one

(52) Childs, L. J.; Pascu, M.; Clarke, A. J.; Alcock, N. W.; Hannon, M. J. *Chem.—Eur. J.* **2004**, *10*, 4291–4300.

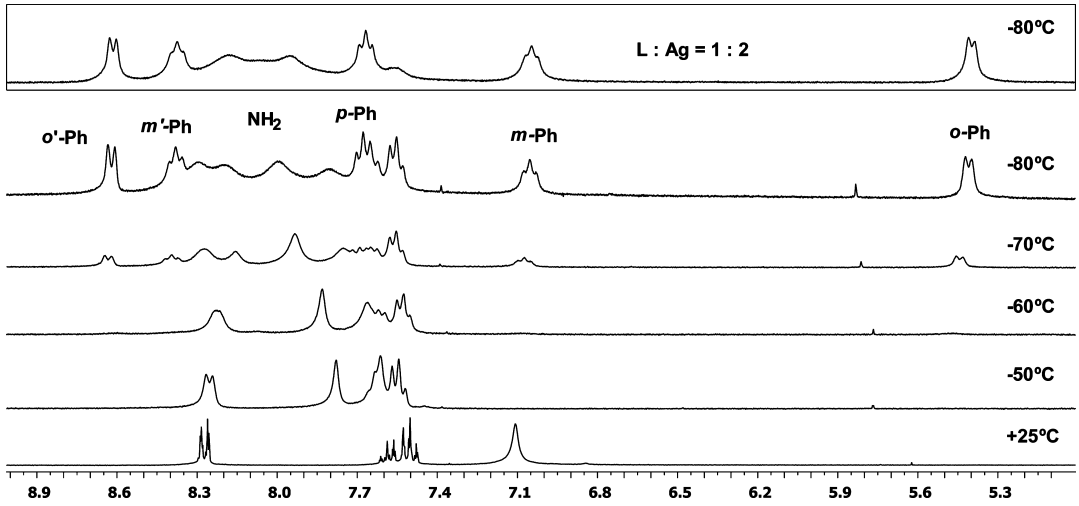

Figure 11. Variable-temperature ^{1}H NMR spectra of **2** in an acetone-d_6 solution. The resonances assigned to the new derivative are indicated. The spectrum inside the rectangle corresponds to a solution with a Phdat/$AgBF_4$ ratio of 1:2 at −80 °C.

meta resonance is overlapped with other resonances). These data indicate that we have detected at low temperatures a defined species that contains an asymmetric aryl group. The spectra recorded at different temperatures are gathered in Figure 11, and it is possible to see that at −70 °C (even at −60 °C) the new species is already present, albeit at a lower concentration. Consequently, the ratio of the new product increases as the temperature is lowered. The most striking feature of these signals is that one ortho proton appears to be highly shielded (5.43 ppm). In order to obtain more information about the structure of the new compound, a series of NMR experiments with derivative **2** were recorded. Given its low solubility (reduced at low temperature), it was not possible to record the ^{13}C or ^{13}C{^{1}H} NMR spectra of **2**, although we were able to determine the chemical shift of the phenylic *C*H resonances at −80 °C with the aid of a g-HMQC experiment. The carbon bonded to the shielded proton appears at 124.2 ppm, a reasonable value for a phenylic carbon. Changes were not observed in the ^{19}F NMR spectrum at −80 °C. The ^{1}H NMR spectra at −80 °C of mixtures Phdat/$AgBF_4$ in 1:2 and 2:1 ratios were also recorded. In the first case, the amount of the new species increased significantly (see spectrum inside the rectangle in Figure 11), while it was reduced for a 2:1 ratio. These results could imply a Ag/L ratio higher than 1 for the new derivative. It is also worth noting that for the shielded proton the coupling constant $^3J_{HH}$ (6.4 Hz) is lower than the $^3J_{HH}$ for the other ortho proton (7.7 Hz) and also lower than that expected for a phenyl ring.

These facts (chemical shift, reduced J_{HH}) can be explained with the following: (i) the existence of an agostic interaction between silver(I) and the C_{Ar}−H bond — however, these interactions are considered not probable for electron-rich metals[4d,38,39,53] — and (ii) the existence of a C−H···Ag hydrogen bond.[4d,38a,39,53] In this case, the shielding of the ortho proton could be due to the anisotropy of an aromatic ring through, for example, a C−H···π interaction.

Although other options such as a η^2 interaction or $\pi-\pi$ stacking cannot be conclusively discarded, they are considered less probable for the following reasons. A η^2 interaction of the $C_{ipso}-C_{ortho}$ bond with the silver center should be associated with more marked changes in the chemical shift of the C_{ortho} atom. The existence of $\pi-\pi$ stacking of the aromatic rings should, in principle, also lead to changes in the chemical shifts of the meta protons and affect in a more similar way the two ortho protons, contrary to the results found in our complex.

Although it is not possible to propose a specific structure for this derivative detected at low temperatures, one possibility is an oligomeric form of complex **7**. In any case, the formation of derivatives with a Ag/L ratio higher than 1 is demonstrated with complex **7**. The extra silver centers could be coordinated to the third nitrogen atom of the triazine ring, to acetone molecules, or to the tetrafluoroborate counteranion as it is observed in complex **7**.

Conclusions

We have demonstrated that the self-assembly of the Ag(I) cation and 2,4-diamino-6-R-1,3,5-triazines (R = phenyl or *p*-tolyl) can give rise to a range of three-dimensional and diverse networks whose precise architecture is R and anion-dependent and where noncovalent interactions play an important role. Hydrogen bonds have been found with the participation in some cases of the triflate oxygen atoms, $\pi-\pi$ stacking, anion−π interactions and Ag···F, CH···Ag, or NH···Ag contacts. Different combinations of these secondary interactions have been found in the distinct type of supramolecules obtained. The $\pi-\pi$ stacking interaction has only been observed in the phenyl derivatives. Some of these supramolecular interactions lead to an increase in the dimensionality from 1D to 3D or from 2D to 3D networks.

When the anion is BF_4^-, with both types of R groups, chiral helical chains with linear silver centers are formed that are interlinked through the anions by secondary interactions to give a 3D structure. The OTf^- counteranion coordinates to the silver atom, which becomes tetracoordi-

(53) Liu, C.-S.; Chen, P.-Q.; Tian, J.-L.; Bu, X.-H.; Li, Z.-M.; Sun, H.-W.; Lin, Z. *Inorg. Chem.* **2006**, *45*, 5812–5821.

nated. In this case, a strong influence of the R group is observed, and a laminar structure or an unusual type of ladder chain is formed. In the triflate derivatives, all of the hydrogen donor or acceptor groups from the triazine ring are involved in hydrogen bonds, and the double N−H···N/N···H−N system found in the free ligands is maintained (amplified to a quadruple bond in the case of the phenyl derivative). A MOF derivative has also been isolated of formula $[Ag_3(Phdat)_2(OH_2)(acetone)_2(BF_4)_3]_n$ whose structure is strikingly similar to that of the complex $[Ag(Toldat)(OTf)]_n$, although the complexes differ in stoichiometry, the anion, and the triazine substituent. The role played by the hydrogen bonding in the latter to build the 3D structure is played by silver centers in the former. In the phenyl derivatives with the BF_4^- or OTf^- anions, a species has been detected at low temperatures that contains an asymmetric phenyl group.

The effect of other counteranions and that of the solvent are under study at this moment.

Further studies are clearly needed in order to evaluate the influence of all factors on the outcome of supramolecular architectures if we hope to understand the self-assembly process and to progress in the field of crystal engineering.

Acknowledgment. This work was supported by the DGES of the Ministerio de Educación y Ciencia of Spain (CTQ2008-03783/BQU) and the Junta de Comunidades de Castilla−La Mancha−FEDER Funds (PCI08-0054-8714). The authors acknowledge Dr. Juan Pedro Andrés and Carlos Rivera from the UCLM for the recording of the X-ray powder diffractograms and thermal analysis.

Supporting Information Available: X-ray crystallographic files (CIF) for **2**, **3**, **5**, **6**, and **7**. Graphics of the TGA and DTA thermal analysis of **2** and **7**. This material is available free of charge via the Internet at http://pubs.acs.org.

IC800997D